Molecular pathobiology for renal tubular dysplasia in Japanese black cattle due to claudin-16 deficiency

黒毛和種牛腎尿細管形成不全症（クローディン-16 欠損症）の分子病態

2006

Hiroshi Ohta

Laboratory of Molecular Medicine, Department of Veterinary Clinical Sciences,
Graduate School of Veterinary Medicine, Hokkaido University

CONTENTS

GENERAL INTRODUCTION

The existence of separate fluid compartments with different molecular compositions is particularly important for the development and maintenance of multicellular organisms. These compartments are delineated by various cellular sheets, which function as barriers to maintain the distinct internal environment of each compartment. Within these sheets, individual cells are mechanically linked with each other to maintain the structural integrity of the sheets, and the intercellular space between adjacent cells is sealed to prevent the diffusion of solutes. Movement of solutes and water through epithelial and endothelial sheets occurs via both the transcellular and the paracellular routes. The major selective barrier of the paracellular pathway is created by the tight junction (TJ) [1, 2]

Tight junctions (TJs) are located at the apicalmost region of lateral membranes of epithelial cells, and play a central role in sealing the intercellular space in epithelial cellular sheets. TJs create the primary barrier to the diffusion of solutes and water through the paracellular pathway and maintain cell polarity as a boundary between the apical and basolateral plasma membrane domains [3-6]. On freeze-fracture electron microscopy, TJs are visualized as a continuous anastomosing network of intramembranous particle strands, *i.e.*, TJ strands, and complementary grooves [7]. The major components of TJ strands are the integral membrane proteins occludin and claudins, all of which have four transmembrane spans and two intervening extracellular loops [8]. Occludin was identified as the first integral membrane protein localized at TJs in chicken [9] and mammals [10]. However, visceral endoderm cells originated from occludin-deficient embryonic stem cells have well-developed networks of TJ strands

[11], and the function of occludin in TJ strands formation are not well understood. More recently, two other transmembrane proteins which do not show any sequence similarity to occludin, claudin-1 and claudin-2, were identified as components of TJ strands [12]. Now, claudins consist of a family of more than 20 homologous subtypes, and they show tissue-specific and segment-specific distribution patterns in epithelia [6, 8] such as those of the gastrointestinal tract [13] and renal tubules [14].

Among these claudin proteins, claudin-16, formerly paracellin-1, has been shown to be responsible for inherited disease. Various mutations of the *CLDN16* gene were reported to be the cause for familial hypomagnesemia with hypercalciuria and nephrocalcinosis (FHHNC) in the human [15]. Simon *et al.* [15] first reported that claudin-16/paracellin-1 was exclusively expressed in the thick ascending limb (TAL) of Henle's loop where reabsorption of Mg^{2+} and Ca^{2+}, for 60 to 70% and 20% of total contents in the glomerular filtrate, respectively, occurred via the paracelluar pathway [16, 17]. Since FHHNC has been characterized by renal Mg^{2+} and Ca^{2+} wasting, claudin-16 is likely to form aqueous pores that function as the paracelluar pathway for Mg^{2+} and Ca^{2+} in claudin-based TJs [15, 18].

Claudin-16 is also responsible for renal tubular dysplasia with interstitial nephritis in Japanese black cattle [19, 20]. This disease is inherited in an autosomal recessive mode and characterized by renal failure, growth retardation, and early death due to renal dysfunction with a high incidence. Affected animals possess a 37-kb or 56-kb deletion in the *CLDN16* gene [19, 21], resulting in the total lack of claudin-16 protein. Kidneys from one-to two-month-old calves affected revealed the presence of immature renal tubules without lumina accompanied by moderate interstitial fibrosis, whereas the numbers and distribution of the glomeruli appeared to be nearly normal. As the animal

grows, the progress of glomerular and tubular atrophy with interstitial fibrosis and lymphocytic infiltration becomes evident [22]. Tubular atrophy, immature glomeruli, and interstitial fibrosis are also observed in the kidneys from FHHNC patients although details have not been reported [23]. These histological findings suggest that the primary lesion of bovine renal dysplasia is an anomalous defect in differentiation of renal tubular epithelial cells and that claudin-16 therefore has some pivotal roles in differentiation and formation of renal tubule segment(s) in addition to the function in paracelluar transport. Interestingly, in contrast to FHHNC, decreases in serum Mg^{2+} and Ca^{2+} concentrations are not apparent in cattle with claudin-16 deficiency, while a reduction in renal reabsorption rate has been suggested for Mg^{2+} [24]. This suggests that there is a compensatory system(s) for metabolism of these divalent cations in the absence of claudin-16 or that bovine claudin-16 may have functions in paracellular transport of Mg^{2+} and Ca^{2+} distinct from those of the human counterpart despite their high homology in amino acid sequences [19, 20].

In human and murine nephron segments, claudin-16 is exclusively expressed in the TAL segment [14, 15], and claudin-16 colocalized with claudin-3, -10 and -11 in this renal segment of murine kidneys [14]. It is possible that the function of claudin-16 alone or in combination with other claudin subtypes, claudin-3, -10, or -11 is essential for renal tubular formation and reabsorption of divalent cations in TAL segment. However, distribution of claudin-16, as well as other claudin molecules, in the bovine nehron segments has not been determined. Hence, to explore the physiological and pathological significance of bovine claudin-16, it is essential to determine the distribution of this claudin subtype, as well as other claudin species, in the bovine kidney, because heterogeneous claudins form individual TJ strands as heteropolymers and claudin

molecules adhere to each other in both homotypic and heterotypic manners [25] at the cell-cell interface to generate consequential variations in the tightness of individual paired TJ strands [26, 27].

Moreover, although histopathological findings on claudin-16-deficient cattle and FHHNC patients indicate some roles of claudin-16 in differentiation and formation of renal tubular segment(s) described above, no information is available about pathology of claudin-16 deficiency in prenatal and neonatal stages. If claudin-16 has some obligatory functions in tubular formation, atrophic and dysplastic lesions would appear in embryonic periods of bovine kidneys lacking claudin-16 and probably begin in the segment where claudin-16 is expressed. Therefore, pathological studies on renal lesions during the periods of renal development are required to clarify the pathogenesis of claudin-16 deficiency. In addition, it is also important to establish *in vitro* model systems that allow us to analyze the function of claudin-16 in paracellular ransport of divalent cations and it's significance in pathogenesis for bovine renal tubular dysplasia.

In this thesis, several studies to investigate these issues were conducted. First, in Chapter I, expression patterns of claudin-16, as well as other major claudin subtypes, in bovine nephron segments were examined by immunofluorescence microscopy. Then, in chapter II, nephrogenesis of claudin-16-deficient bovine fetuses was histologically analyzed to reveal whether elimination of claudin-16 affected the renal tubular development in utero. Third, in chapter III, the usefulness of murine metanephroi organ culture system in analyzing the roles of claudins, including claudin-16, in paracellular ransport and in renal development was evaluated. Some parts of this work were published as follows:

1) Ohta, H., Adachi, H., Takiguchi, M. and Inaba, M. Restricted localization of claudin-16 at the tight junction in the thick ascending limb of Henle's loop together with claudins 3, 4, and 10 in bovine nephrons *J. Vet. Med. Sci.* (in press).

2) Ohta, H., Adachi, H. and Inaba, M. Developmental Changes in the expression of tight junction protein claudins in murine metanephroi and embryonic kidneys. *J. Vet. Med. Sci.* (in press).

Another manuscript entitled "Morphologically normal formation of nephrons in CLDN16-/- bovine fetuses with postnatal development of renal tubular dysplasia" (Ohta, H., Ito, D., Otuka, Y., Kageyama, S., Hirayama, H., Onoe, S., Umemura, T., and Inaba, M.) has been submitted for publication.

CHAPTER I

Restricted localization of claudin-16 at the tight junction in the thick ascending limb of Henle's loop together with claudin 3, 4, and 10 in bovine nephrons

INTRODUCTION

To explore the physiological and pathological significance of bovine claudin-16 in renal tubular formation and reabsorption of divalent cations, it is essential to determine the distribution of this claudin subtype in the bovine kidney. In addition, it is also important to determine the expression and distribution of other claudin species in the segment to which claudin-16 is localized, because heterogeneous claudins form individual TJ strands as heteropolymers and claudin molecules adhere to each other in both homotypic and heterotypic manners [25] at the cell-cell interface to generate consequential variations in the tightness of individual paired TJ strands [26, 27]. A distribution pattern of claudin-16 restricted to the TAL, consistent with the situation in the human kidney [15], was also demonstrated in mouse nephron segments where several other claudin isoforms, including claudin-3, -10, and -11, were also found in TJs together with claudin-16 [14]. However, no information about claudin-16 in the bovine kidney has been available till date.

In this chapter, studies were conducted to examine expression of claudin-16 and several other major claudin subtypes, claudins 1-4 and 10, in specified tubular segments of normal bovine kidneys by immunofluorescence microscopy using antibodies specific to each claudin subtypes and segment marker proteins. Care was taken to ensure the specificities of the antibodies to claudins 16 and 1-4 by utilizing fusion proteins to confirm the disappearance of specific reactions when present. The results obtained demonstrate that claudin-16 has a distribution restricted to the tight junction in a specific tubular segment along with some other claudin subtypes.

MATERIALS AND METHODS

Tissue collection and preparation

Kidneys were obtained from 7months old healthy Japanese black cattle that were determined to be free of type-1 and type-2 *CLDN16* mutations by the methods described previously [19, 21] in our laboratory and cut into slices. Slices were frozen in liquid nitrogen with or without OCT compound (Sakura Finetechnical Co., Tokyo, Japan) for immunohistochemistry and RNA analyses, respectively.

Antibodies

Rabbit anti-bovine claudin-16 polyclonal antibody (pAb) was kindly provided by Drs. Akiko Takasuga and Yoshikazu Sugimoto (Shirakawa Institute of Animal Genetics, Fukushima, Japan). Rabbit pAbs to human claudin-1, -2, -3, -10, and -11 and mouse monoclonal antibody (mAb) to human claudin-4 and occludin were purchased from Zymed Laboratories (South San Francisco, CA, USA). Rabbit anti-aquaporin-1 (AQP1), anti-chloride channel-K (CLC-K), anti-Tamm-Horsfall glycoprotein (THP), and goat anti-AQP2 pAbs were purchased from Chemicon International (Temecula, CA, USA), Alomone Laboratories (Jerusalem, Israel), Biomedical Technologies (Stoughton, MA, USA), and Santa Cruz Biotechnology (Santa Cruz, CA, USA), respectively. Rabbit anti-rat thiazide-sensitive Na-Cl cotransporter (NCCT) pAb [28] was kindly provided by Dr. M. A. Knepper (Laboratory of Kidney and Electrolyte Metabolism, National Institute of Health, Bethesda, MD, USA). Rabbit anti-dog Na, K-ATPase pAb was described previously [29].

cDNA cloning and construction of plasmids

Total RNA was extracted from bovine liver, kidney, and small intestine using the SV total RNA isolation system (Promega, Madison, WI, USA). First strand cDNA was synthesized using 1 μg of total RNA in the SuperScript™ first-strand synthesis system for RT-PCR (Invitrogen, Gaithersburg, MD, USA). cDNA fragments for bovine claudin-1, -2, -3, and -4 were amplified by RT-PCR using primers designed based on cDNA fragments of human or murine counterparts. The amplified cDNAs were cloned into pCR II-TOPO vector using a TOPO TA clonig kit (Invitrogen), and the nucleotide sequences were determined using a CEQ™ 8800 DNA analysis system (Beckman Coulter, Fullertion, CA, USA). We searched the GenBank database for partial cDNA sequences, and found 13 independent bovine expressed sequence tag (EST) clones possessing nucleotide sequences identical to those obtained for bovine claudins 1-4. The EST clones were CB454425, CB455833, and BF040486 for claudin-1, AV604013, AV605969, BE480970, and BE667438 for claudin-2, CB419176, CB445175, and CB454984 for claudin-3, and BF073399, BI775226, and CK944271 for claudin-4. Since these overlapping clones appeared to contain the entire coding region of each claudin molecule, we amplified cDNAs for coding regions by PCR using primer pairs prepared based on the sequences of appropriate EST clones (Table 1). The amplified cDNAs were cloned into pCR II-TOPO vector and the sequences were determined. To generate recombinant proteins of the C-terminal cytoplasmic domains of bovine claudins 1-4 and 16 fused to glutathione S-transferase (GST), the corresponding nucleotide sequences of bovine claudins were amplified by PCR, cloned into pGEX-6P-1 vector (Amersham Biosciences, Piscataway, NJ, USA), and the recombinant proteins were isolated by affinity purification with glutathione-uniflow

resin (Clontech, Palo Alto, CA, USA).

Sodium dodecyl sulfate-polyacrylamide gel electrophoresis (SDS-PAGE) and immunoblotting

GST-fusion proteins of the cytoplasmic portions of bovine claudin species were subjected to SDS-PAGE. Separated proteins were stained with Coomassie brilliant blue R-250 or transferred to a polyvinylidene difluoride membrane followed by immunoblotting for detection of claudin polypeptides using the ECL chemiluminescence detection system (Amersham Biosciences, Buckinghamshire, UK).

Immunofluorescence microscopy

Pairs of serial 7μm frozen sections of the kidney were prepared. One of the sections was incubated with the appropriate anti-claudin pAb and the other was reacted with a pAb to one of the segment markers. For the control experiment, the anti-claudin antibody was incubated with excess amounts of appropriate GST-fusion proteins containing the C-terminal cytoplasmic peptide prior to incubation with tissue sections. Sections were then washed three times with phosphate-buffered saline (PBS), followed by incubation for 30 min with secondary antibodies conjugated with AlexaFluor 568 or 488 (Molecular Probes, Inc., Eugene, OR, USA). After washing with PBS, sections were embedded in ProLong antifade reagent (Molecular Probes, Inc.) and examined under an ECLIPSE E800 microscope (Nikon, Tokyo, Japan) or a Zeiss LSM 5 PASCAL confocal laser-scanning microscope (Carl Zeiss Japan, Tokyo, Japan). In some experiments, tissue sections were double-stained with anti-claudin-4 mAb and the appropriate pAb (Fig. 4).

Individual nephron segments were identified by the use of antibodies to marker proteins specific to each segment based on previous studies: AQP1 for proximal tubules and thin descending limbs [30], CLC-K for thin ascending limbs [31, 32], THP for the TAL [33], NCCT for distal convoluted tubules [28], and AQP2 for collecting ducts [34].

RESULTS

Cloning of cDNAs encoding bovine claudins 1-4, specificities of antibodies and detection of claudin proteins

To prepare expression plasmids and GST-fused proteins for judging the specificities of commercially available antibodies to bovine claudins, we newly isolated cDNAs encoding major claudins 1-4.

The amino acid sequences of bovine claudins 1-4 deduced from their cDNAs are shown in Fig. 1A with that of bovine claudin-16, and are highly homologous to those of their human and murine counterparts. The molecular masses of claudins 1-4 and 16 are 22.8, 24.5, 23.3, 22.1, and 26.1 kDa, respectively. Multiple sequence alignments (Fig. 1A) also indicated that the amino acid sequences of the C-terminal cytoplasmic tail, the region used as the antigen for production of antibodies, were fairly diverse among different bovine claudin species.

Immunoblotting analysis of the GST-fused C-terminal tail regions of claudin-1~-4 and -16 (GST-claudin-16Ct, etc.) demonstrated that each antibody used in this study specifically recognized the corresponding claudin subtype (Fig. 1B). In immunofluorescence microscopy, claudin-16 protein was found as lines or dots near the apical surface of tubular epithelial cells, consistent with signals for occludin, a ubiquitous TJ protein, demonstrating that claudin-16 colocalized with occludin at the TJ (Fig. 1C). Fluorescent signals were specific to claudin-16, since the signals disappeared when sections were reacted with the anti-claudin-16 pAb in the presence of GST-claudin-16Ct but not in the presence of GST alone. Likewise, specificities in reactivity of antibodies to claudins 1-4 were also verified (data not shown).

Segment-specific expression of claudin-16 and claudins 1-4 and 10 in bovine nephrons

Expression of claudin-16 in different tubular segments was examined by immunofluorescence microscopy (Fig. 2). Because of the limited availability of antibodies to segment-specific marker proteins applicable to double staining of the tissue section in combination with the antibody to each claudin subtype, most of the present studies on distribution of claudins were performed on pairs of serial frozen sections, one of which contained the tubular segments corresponding to those in the other section. One of the sections was reacted with the appropriate anti-claudin antibody and the other one was stained for the marker protein.

In the cortex, claudin-16 was found at the cell-cell junctional areas of epithelial cells in some tubules. Tubular segments carrying positive signals of AQP1, NCCT, or AQP2, that is proximal tubules, distal convoluted tubules, and collecting ducts, respectively, had no specific signals corresponding to claudin-16 (Figs. 2A, 2E, and 2F). In contrast, tubules with positive signals for THP and claudin-16 on serial sections were coincident with each other, indicating that claudin-16 was expressed in the TAL region (Fig. 2D). In the medulla, some tubules exhibited distribution of claudin-16 at the apical regions of epithelial cells. These tubules were positive for THP, but were negative for AQP1 (Fig. 2B), CLC-K (Fig. 2C), and AQP2 (data not shown), indicating that claudin-16 was present in the TAL segment but not in thin descending and ascending limbs of Henle's loop and collecting ducts.

The expression and distribution of claudins 1-4 and 10 were also analyzed. As demonstrated in Fig. 3A, claudin-1 was concentrated at the apical regions of epithelial

cells of Bowman's capsule. Claudin-2 was localized at both the apical and basolateral regions of epithelial cells of AQP1-positive tubules in the cortex (Fig. 3B) and medulla (Fig. 3C), that is, the proximal tubule and thin descending limb, respectively. Claudin-3 was detected in epithelial cells of Bowman's capsule (Fig. 3D) as observed for claudin-1. Claudin-3 was also detected at the TJ region in the distal nephron involving the TAL, distal convoluted tubules, and collecting ducts, which were positive for THP, NCCT, and AQP2, respectively (Figs. 3E-3G). Moreover, claudin-4 was found in distal nephrons including CLC-K-positive tubules in the inner medulla (thin ascending limb), the TAL, distal convoluted tubules, and collecting ducts with both apical and basolateral distributions in all of these segments (Figs. 3H-3K). All the signals for claudins 1-4 disappeared or were markedly reduced to the background level in the serial sections reacted with each antibody in the presence of the appropriate GST fusion proteins described above, indicating that the signals obtained were specific to each claudin subtype.

In addition, claudin-10 was visualized at the apical side of epithelial cells of the tubules positive for AQP1 in the medulla (Fig. 3L) but not in the cortex (data not shown). Claudin-10 was also detected in the cells of THP-positive tubules with apicalmost distribution (Fig. 3M). These findings indicated the presence of claudin-10 in the thin descending limb and the TAL of Henle's loop, although we found no evidence to show specificity in reactivity of the anti-claudin-10 with bovine counterpart. We could not detect immunofluorescent signals for claudin-11, a claudin subtype that has been shown to localize in the TAL of mouse nephrons [14], when the sections were reacted with an anti-claudin-11 antibody that exhibited weak but significant signals in mouse tissues (data not shown). These data are summarized and compared with the

previously reported segment-specific distributions of corresponding claudins in mouse nephrons [14] in Fig. 5.

Claudins expressed in TAL of Henle's loop

The data reported above indicated that bovine claudins 3, 4, and 10 were present at the TJ area in epithelia of the TAL segment where claudin-16 was expressed, although claudin-4 had both apical and basolateral localization (Figs. 3H-3K). This is inconsistent with the previous observation that TJ in the TAL region are comprised of claudins 3, 10, 11, and 16 but not claudin-4 in mouse nephrons [14]. To confirm our observation for bovine tissues, colocalization of claudin-4 with other subtypes was analyzed by double staining on the same frozen section. Immunofluorescence detection of claudin-16 and claudin-4, shown in Fig. 4A, confirmed that claudin-4 colocalized with claudin-16 at the apical regions of epithelial cells in the tubules positive for THP, the TAL segment. Likewise, immunofluorescent signals of claudin-4 were partly merged with those of claudin-3 or -10 at the apical regions of the cells in the TAL (Figs. 4B and 4C). Disagreement of the signals between claudin-4 and other claudins appeared to reflect dispersed distribution of claudin-4 at the basolateral domain that was demonstrated by colocalization of Na,K-ATPase, a typical enzyme present in the basolateral membranes, with claudin-4 (Fig. 4D).

Table 1. Primers used to isolate cDNA clones for bovine claudins 1-4

Nucleotide sequences of primer pairs to isolate cDNA clones for coding regions of bovine claudins 1-4 and the GenBank accession numbers of the EST clones containing the primer sequences are presented.

Subtype	Sequence	EST clone
Claudin-1	Forward, 5'-TGCACCTGCTGCCCCTGAGCC-3'	CB454425
	Reverse, 5'-ATTCCTTACGATAGAGGGGAG-3'	CB455833
Claudin-2	Forward, 5'-GAAATGAGGGATTAGAGGCCG-3'	AV604013
	Reverse, 5'-TGGCTTCTGGAGGGGGGGTGG-3'	BE667438
Claudin-3	Forward, 5'-CGCCGCCCTTGTGTCCGTCCG-3'	CB419176
	Reverse, 3'-GAGGAGGGCTAGCAGCTGGGG-3'	CB454984
Claudin-4	Forward, 5'-TGCGAAGTAGCCGTCCGCGGC-3'	BF073399
	Reverse, 5'-CCATGGTCCACTGAGCACCCACTC-3'	BI775226

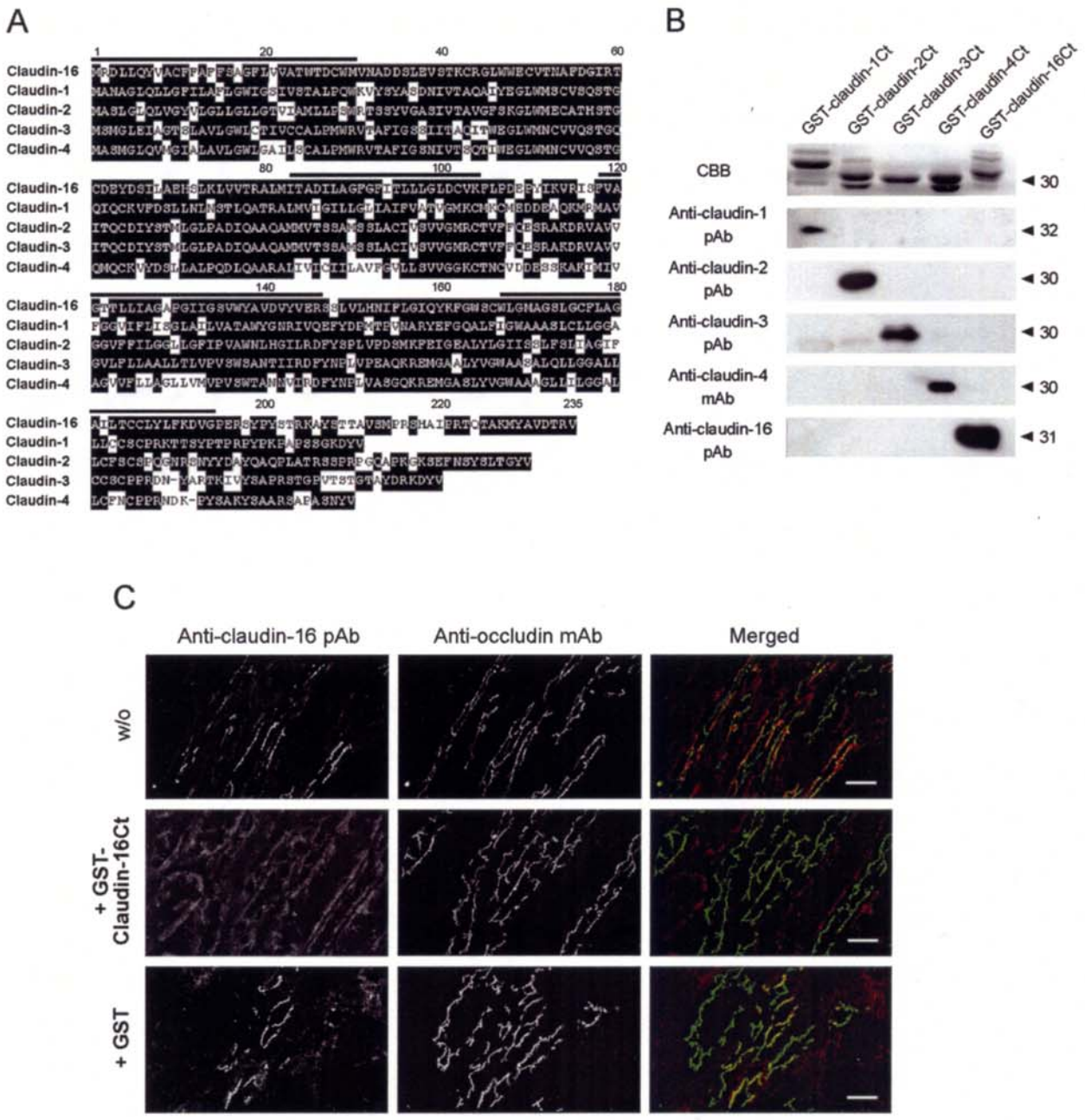
A
Claudin-16
Claudin-1
Claudin-2
Claudin-3
Claudin-4
B
GST-claudin-1Ct
GST-claudin-2Ct
GST-claudin-3Ct
GST-claudin-4Ct
GST-claudin-16Ct
CBB
Anti-claudin-1 pAb
Anti-claudin-2 pAb
Anti-claudin-3 pAb
Anti-claudin-4 mAb
Anti-claudin-16 pAb
30
32
30
30
30
31
C
Anti-claudin-16 pAb
Anti-occludin mAb
Merged
w/o
+ GST-Claudin-16Ct
+ GST

Figure 1. Amino acid sequences and detection of bovine claudins. A, amino acid sequences of bovine claudin-16 and claudins 1-4 deduced from their cDNA sequences are presented. Bars indicate putative membrane-spanning regions depicted based on previous reports [8]. Amino acid residues of each claudin subtype that are conserved among cattle, humans, and mice are highlighted with black backgrounds. The amino acid sequences of C-terminal cytoplasmic domains are fairly diverse. The nucleotide sequences of cDNA for bovine claudins 1-4 determined in the present study have been deposited in the GenBank with accession numbers AB178476, AB115779, AB115781, and AB185928 for claudins 1-4, respectively. B, immunoblotting analysis of GST-fused C-terminal peptides of claudin-16, and claudins 1-4 (GST-claudin-16Ct, etc.). GST-fused recombinant proteins were separated by SDS-PAGE followed by staining with the Coomassie brilliant blue (CBB) or immunoblotting with appropriate antibodies. Apparent molecular masses of each protein are indicated in kDa. C, immunofluorescence detection of bovine claudin-16 in kidney cryosections with anti-claudin-16 pAb. Frozen sections were reacted with the anti-claudin-16 pAb (red) and anti-occludin mAb (green) in the absence (*w/o*) and presence of GST-claudin-16Ct (*+GST-claudin-16Ct*) or GST alone (*+GST*). Merged images represent colocalization of claudin-16 and occludin (*w/o* and *+GST*). Bars = 20 μm.

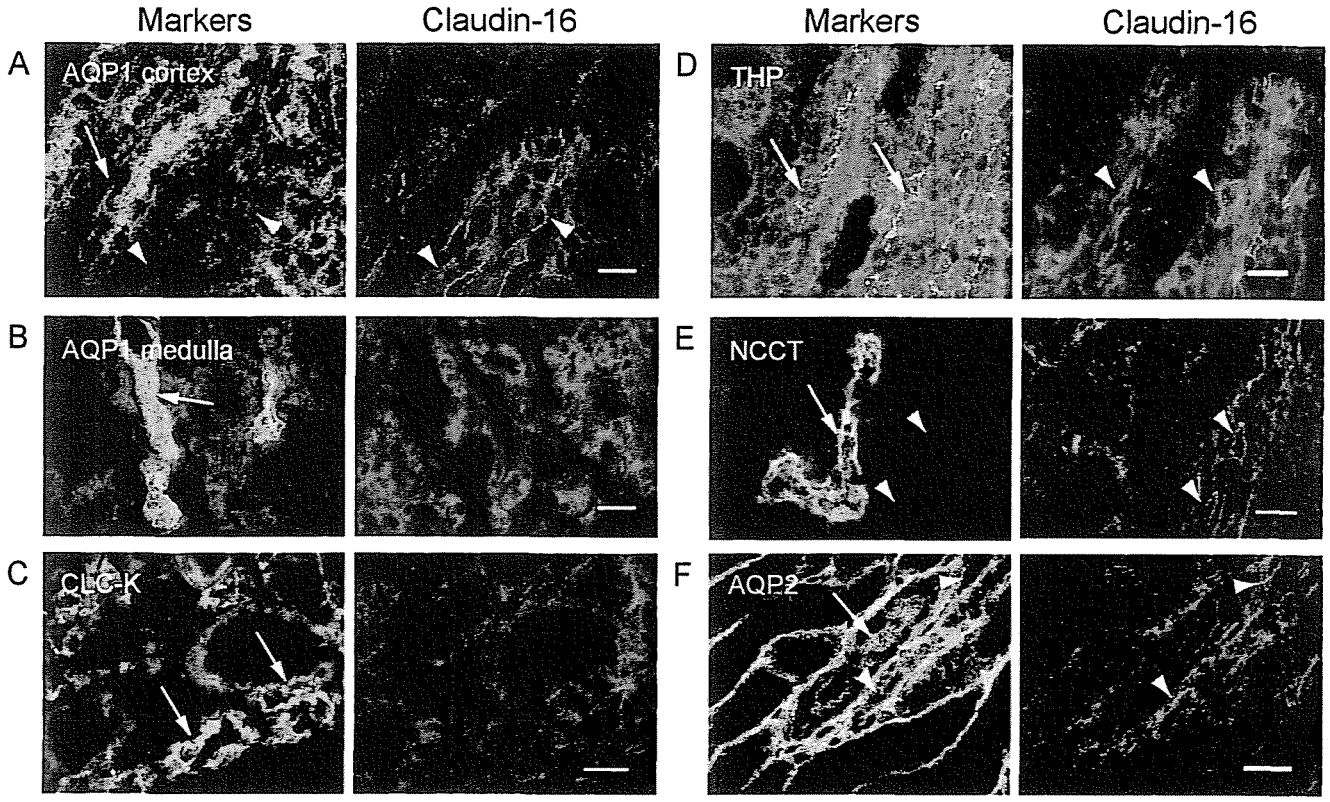

Figure 2. Segment-specific expression pattern of claudin-16 in bovine nephrons. One of each pair of serial frozen sections was reacted with the pAb for segment markers, AQP1 (*A* and *B*), CLC-K (*C*), THP (*D*), NCCT (*E*), and AQP2 (*F*), and the other was visualized with the anti-claudin-16 pAb (*Claudin-16*). Although the anti-AQP2 pAb used in this study gave immunospecific signals when reacted with murine renal tissue sections, it showed unexpected staining of connective tissues of basement membranes in frozen sections from bovine kidneys presumably due to some non-specific reactions. Specific staining by this AQP2 pAb is observed at the apical surface of some tubules with relatively large lumen, the collecting duct. (F, also see Fig. 3G and 3K). Arrows indicate tubules identified with segment markers and arrowheads indicate signals of claudin-16 and corresponding regions in the section for marker proteins. Scale bars = 20 μm.

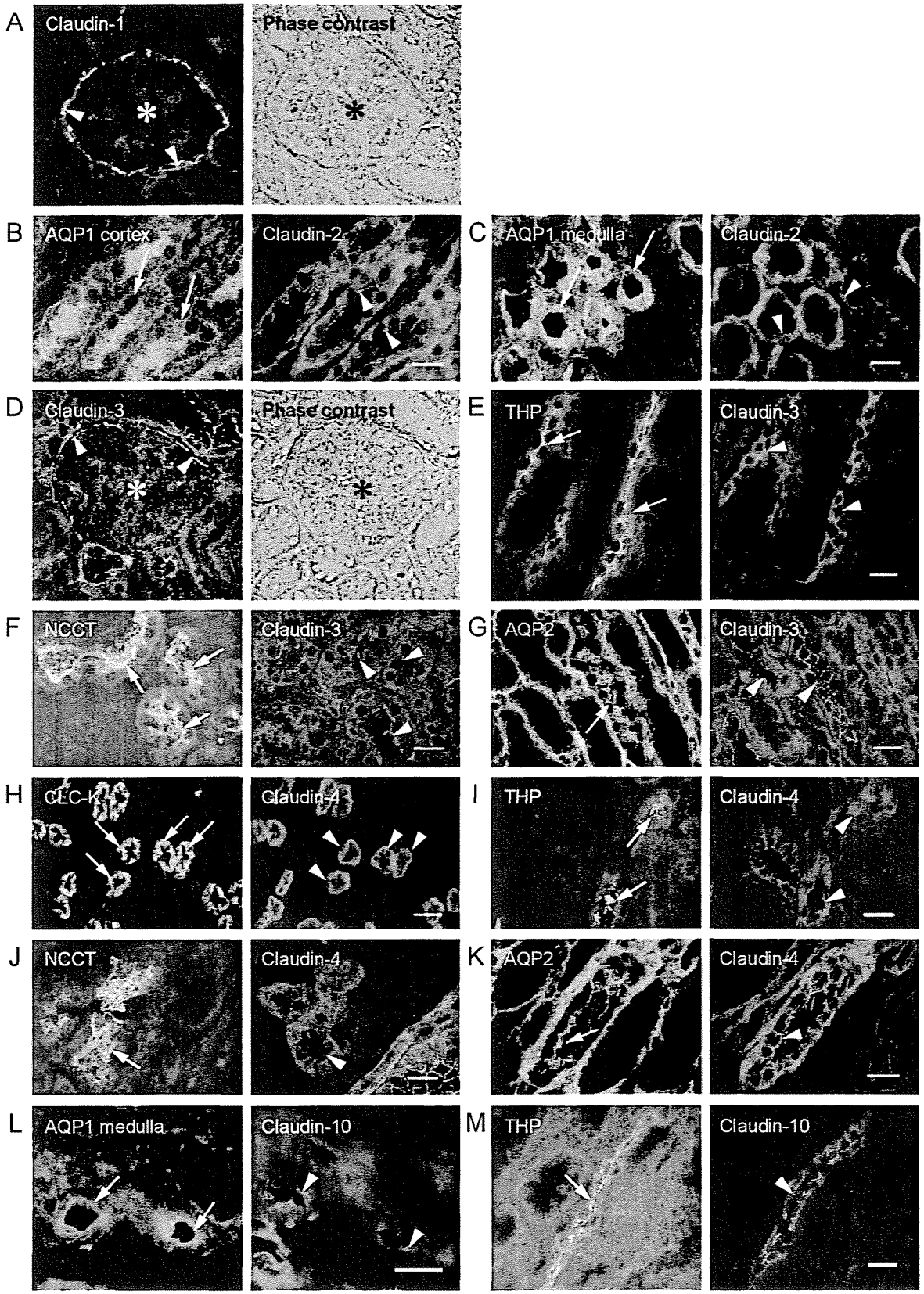
A
Claudin-1
Phase contrast
B
AQP1 cortex
Claudin-2
C
AQP1 medulla
Claudin-2
D
Claudin-3
Phase contrast
E
THP
Claudin-3
F
NCCT
Claudin-3
G
AQP2
Claudin-3
H
CLC-K
Claudin-4
I
THP
Claudin-4
J
NCCT
Claudin-4
K
AQP2
Claudin-4
L
AQP1 medulla
Claudin-10
M
THP
Claudin-10

Figure 3. Segment-specific expression of claudins 1-4 and 10 in bovine nephrons. Claudins 1-4, 10 and segment markers were detected by immunofluorescence microscopy in serial frozen sections. To reveal the presence of claudin-1 and claudin-3 in Bowman's capsules, corresponding phase-contrast images are shown (*A* and *D*). Asterisks indicate glomeruli. Arrows and arrowheads indicate signals for marker proteins and claudins, respectively. Bars = 20 μm.

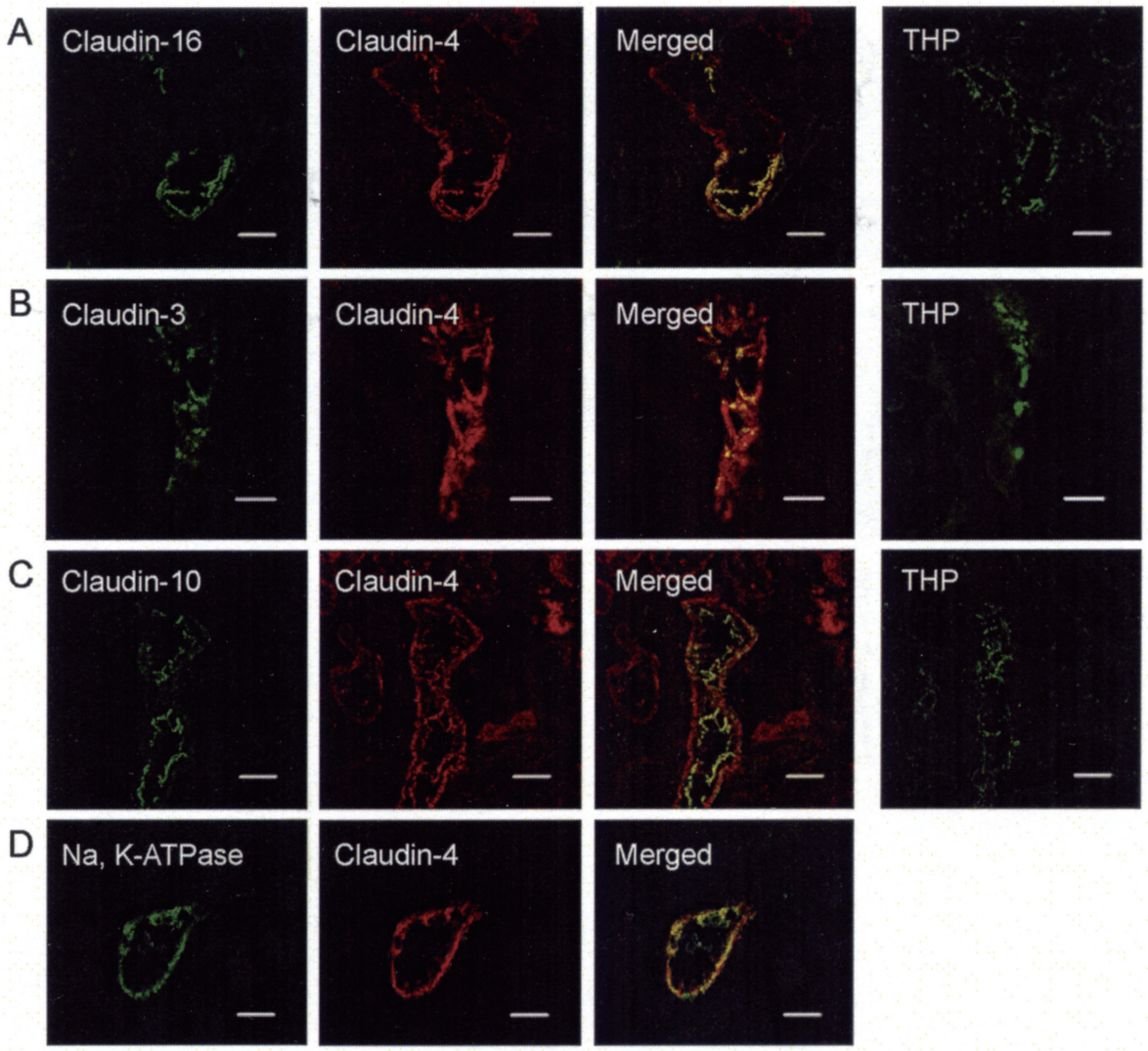

Figure 4. Localization of claudin-16, -3, -4, and -10 in TAL segments. One of the serial frozen sections was reacted with the anti-THP pAb to detect the TAL segment (*A-C*, right panels). The other section was double-stained with the anti-claudin-4 mAb and the anti-claudin-16 pAb (*A*), anti-claudin-3 pAb (*B*), or anti-claudin-10 pAb (*C*). Merged images show that claudin-16 colocalizes with claudin-4 at TJ region of the TAL segment (*A*). Colocalization of claudin-4 with claudin-3 and -10 at TJ region of the TAL are also demonstrated (*B* and *C*). The frozen section was also reacted with anti-claudin-4 mAb and anti-Na,K-ATPase pAb to show colocalization of claudin-4 with Na,K-ATPase at basolateral membranes (*D*). Bars = 20 μm.

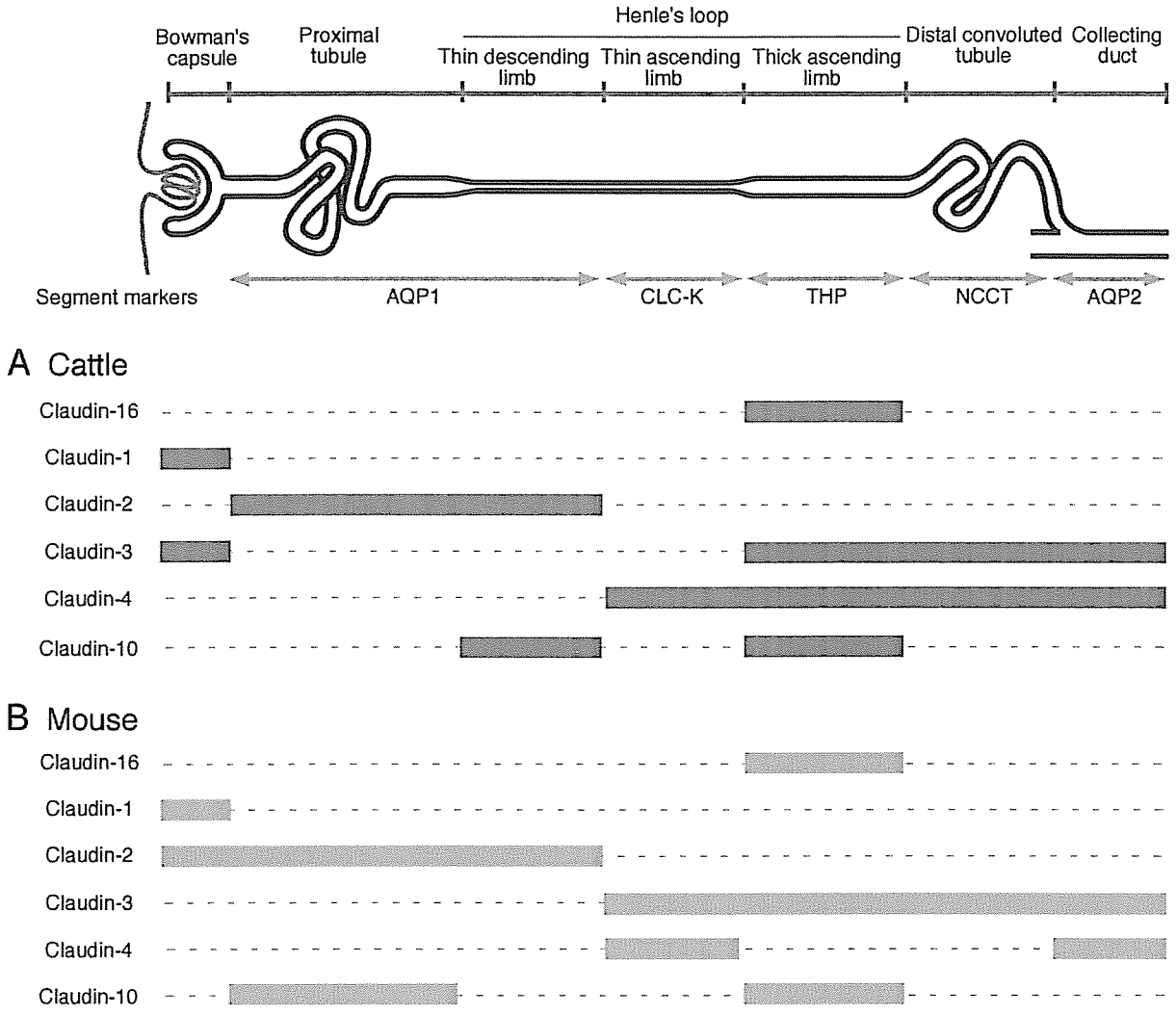

Figure 5. Summary of the segment-specific expression of claudins 1-4, 10, and 16 in the bovine nephron. Tubular segments, marker proteins for each segment, and distribution of claudins 1-4, 10, and 16 (indicated by closed boxes) determined in the present study for the bovine nephron are summarized and compared with those for the mouse nephron (14).

DISCUSSION

The present study demonstrated that the expression and distribution of bovine claudin-16 were exclusively limited to the renal tubular segment TAL (Fig. 2) as has been reported for the human [15] and mouse [14].

Claudin-16/paracellin-1 was first identified as the product of the gene (*CLDN16/PCLN1*) responsible for FHHNC in humans [15] followed by the observation that renal tubular dysplasia in cattle was linked to deleterious mutations of the *CLDN16* gene [19, 20]. Although the significance of claudin-16 function in Mg^{2+} and Ca^{2+} metabolism remains uncertain in cattle [24], the affected animals [22] and FHHNC patients [23] share several histopathological findings, including tubular atrophy, immature tubules, and interstitial fibrosis. These renal lesions are observed in affected animals with claudin-16 deficiency at 1 to 2 months of age, and appear to progressively lead to decreases in the number of glomeruli [22]. These observations suggest that the barrier function in the paracelluar pathway, function in cell-cell adhesion, or both of claudin-16 in the TAL segment are important in the differentiation, formation, and/or maintenance of renal tubules. The expression of claudin-16 restricted to the TAL segment found in this study indicates that the renal dysplasia is consequential to dysfunction of TAL epithelial cells due to the lack of claudin-16. Pathological studies on developing kidneys of affected animals in prenatal and neonatal periods are required.

A previous study on the murine kidney [14] showed that claudin-3, -10, and -11 were present at TJ in epithelial cells of the TAL segments in addition to claudin-16. We could not detect claudin-11, as described above, but instead found the distribution of claudin-4 at the TJ in this segment of the bovine kidney, in contrast to its absence in the

TAL of the mouse nephron. It is unlikely that the anti-claudin-11 antibody used in the present study reacted with mouse claudin-11 but not with the bovine one, since bovine and mouse claudin-11 share an identical C-terminal amino acid sequence (GenBank accession numbers BC105204 and NM_008770, respectively) to which the antibody was raised. Rather, the absence of the signals for claudin-11 in bovine tissues may be explained by the extremely low levels of expression of this claudin subtype in adult kidneys compared with fetal tissues that was demonstrated by RT-PCR (see Chapter II). Actually, weak but significant immunofluorescent signals for claudin-11 were observed at the apical side of some tubules in developing kidneys from a bovine fetus at embryonic days 100 (data not shown). Thus, we conclude that claudin-16, -3, -4, and -10 are the major components of TJ strands of TAL regions in adult bovine kidneys (Fig. 5).

The present study also showed that the bovine kidney had a segment-specific expression pattern for claudins that was basically the same as that observed for mouse kidneys but with some discrepancies (Fig. 5). First, as described above, this study showed that bovine claudin-4 was found throughout the distal nephron, while it was present in the thin ascending limb of Henle's loop and the collecting duct in the mouse kidney [14]. In these segments, bovine claudin-4 showed distribution both at the TJ and the basolateral membranes. Many investigators have reported basolateral distribution of some claudins, including claudin-4 [13, 35-37], although the precise roles of claudins in the plasma membrane compartment other than TJ remain unknown; they may simply represent a storage pool capable of being recruited to the TJ when required, or they may have some novel functions in intercellular adhesion and/or adhesion between cells and the extracellular matrix.

Distributions of claudin-2 and -3 showed differences between cattle and mice. Claudin-2 was absent but claudin-3 was present in Bowman's capsule in the bovine kidney (Fig. 3), whereas the former, but not the latter, was found there in mice [14]. Since Bowman's capsule contains claudin-1 in both bovine and mouse kidneys (Fig. 5), and claudin-3 strands but not claudin-2 strands can interact with claudin-1 strands [25], there may be some differences between cattle and mice in the permeability of the TJ in Bowman's capsule although no substantial information about the paracellular pathway in this part is available. Furthermore, bovine claudin-3 was observed in the TAL, distal convoluted tubules, and collecting ducts, but exhibited no signal in the thin ascending limb, although it was found in all of these segments in the mouse [14]. The anti-CLC-K antibody used in this study detects both CLC-K1 and CLC-K2, and recognizes whole distal nephron segments, including the thin ascending limb [31, 32]. Thus, our conclusion that the thin ascending limb lacks claudin-3, is based on the absence of immunofluorescence signals for claudin-3 in the tubules stained positively with the anti-CLC-K antibody in the inner medulla. These differences in segment-specific distribution of claudins 1-4 may give us relevant information about physiological functions of renal tubules characteristic to different animal species, as previous studies demonstrated that some claudins, including claudin-1 [38, 39] and -4 [40] had low-conductance characteristics, whereas claudin-2 likely constituted aqueous pores with high conductance [26].

In conclusion, the present study shows that the bovine kidney has a segment-specific distribution pattern for claudin-16 and claudins 1 through 4 and 10, suggesting distinct characteristics of the TJ concerned. The expression of claudin-16 is exclusively restricted to the TJ in the TAL region where claudins 3, 4, and 10 colocalize,

indicating that the aberrant lesions found in renal dysplasia in Japanese black cattle are subsequent to some undefined events in this restricted area, the TAL, due to the total lack of claudin-16.

SUMMARY

Claudin-16 is one of the tight junction protein claudins and has been shown to contribute to reabsorption of divalent cations in the human kidney. In cattle, total deficiency of claudin-16 causes severe renal tubular dysplasia without aberrant metabolic changes of divalent cations, suggesting that bovine claudin-16 has some roles in renal tubule formation and paracellular transport that are somewhat different from those expected from the pathology of human disease. As the first step to clarify these roles, we examined the expression and distribution of claudin-16 and several other major claudin subtypes, claudins 1-4 and 10, in bovine renal tubular segments by immunofluorescence microscopy. Claudin-16 was exclusively distributed to the tight junction in the tubular segment positive for Tamm-Horsfall glycoprotein, the thick ascending limb (TAL) of Henle's loop, and was found colocalized with claudins 3, 4, and 10. This study also demonstrates that bovine kidneys possess segment-specific expression patterns for claudins 2-4 and 10 that are different from those reported for mice. Particularly, distribution of claudin-4 in the TAL and distal convoluted tubules was characteristic of bovine nephrons as were differences in the expression patterns of claudins 2 and 3. These findings demonstrate that the total lack of claudin-16 in the TAL segment is the sole cause of renal tubular dysplasia in cattle and suggest that the tight junctions in distinct tubular segments including the TAL have barrier functions in paracellular permeability that are different among animal species.

CHAPTER II

Morphologically normal formation of nephrons in *CLDN16*$^{-/-}$ bovine fetuses with postnatal development of renal tubular dysplasia

INTRODUCTION

The most characteristic features of bovine claudin-16 deficiency are renal tubular dysplasia with mononuclear cell infiltration [22, 41]. The pathological change was reported to be apparent in the affected calves at one month of age [22]. The kidneys from one-to two-month-old calves affected revealed the disarrangement of renal tubules and tubular atrophy accompanied by moderate interstitial fibrosis and mild mononuclear cell infiltration without glomerular lesions [22]. Tubular atrophy, immature glomeruli, and interstitial fibrosis are also observed in the kidney from FHHNC patients although details have not been reported [23]. These findings suggest that the primary lesion in claudin-16-null animals is the defect in renal tubular development and that claudin-16 has some pivotal roles in differentiation and formation of renal tubule segment(s) in addition to the function in paracellular transport. If this assumption is correct, atrophic and dysplastic lesions would appear in fetal periods and probably begin in the TAL segment where claudin-16 is exclusively expressed, as demonstrated in Chapter I. However, no information about renal pathology in the fetal and postnatal stages is available till date.

The purpose of the present study is to examine if claudin-16 deficiency would cause abnormal renal tubular formation in the fetal stage of the affected animals. Here, fetuses homozygous for the type-1 claudin-16 deficiency of several distinct embryonic days were generated by embryonic transfer, and histological analysis was performed on *in utero* development of renal tubules. The analysis also included the expressions of the TJ proteins, including various claudin subtypes reported to have segment-specific distributions in murine renal tubules [14], by RT-PCR, immunoblotting, and

immunofluorescence microscopy. Particularly, expression of claudin-3, -4, and -10 which were defined as the major constituents of TJ strands in the TAL segment as well as claudin-16, as shown in Chapter I, was carefully examined.

MATERIALS AND METHODS

Generation of claudin-16-deficient fetuses and sample collections

The embryos that had been judged as homozygous for the type-1 mutation of the *CLDN16* gene were transferred into recipient cows at 7-9 days after estrus as previously reported [42]. The fetuses were obtained by the caesarean operation, at 100, 180, and 270 days of gestation (E100, E180, and E270, respectively). Kidneys of fetuses were removed and cut into slices. Slices were fixed in 4% paraformaldehyde, or frozen in liquid nitrogen with or without OCT compound (Sakura Finetechnical Co.) for immunohistochemistry and analyses of RNA and proteins, respectively. The procedure for animal handling was approved by the Hokkaido Animal Research Center. Kidneys were also obtained from normal fetuses on embryonic day 100 and 140 (E100 and E140, respectively) and from a neonate at 2 days after birth (P2). Kidneys were also obtained from claudin-16-deficient and normal animals at 7 months of age.

The genomic DNAs were extracted from peripheral blood leukocytes or livers of the animals examined using QIAmp blood mini kit or QIAmp DNA mini kit (QIAGEN, MD, USA). Genotyping of embryos and fetuses for the type-1 *CLDN16* gene mutation was carried out as described previously [19, 42]. The genotypes determined are designated as $CLDN16^{-/-}$ and $CLDN16^{+/+}$ for homozygous for and free from the type-1 mutation, respectively.

Antibodies

Antibodies to TJ proteins were described in Chapter I. A rabbit anti-Tamm-Horsfall glycoprotein (THP) pAb and mouse anti-β-actin mAb were purchased from Biomedical

Technologies (Stoughton, MA, USA) and Sigma (St. Louis, MO, USA), respectively.

The specificities of signals in immunoblotting and immunofluorescence microscopy for claudins 1-4 and 16 were verified using GST-tagged recombinant proteins containing the C-terminal region of each claudin as described above (Chapter I).

RT-PCR and immunoblotting of tight junction proteins in bovine kidneys

RT-PCR. Total RNA was isolated from kidneys using a SV total RNA isolation system (Promega). Reverse transcription was performed with 1 μg of total RNA using SuperScript first-strand synthesis system (Invitrogen). RT-PCR for detection of claudins 1-4, 10, 11 and 16, occludin, ZO-1, and glyceraldehyde 3-phosphate dehydrogenase (GAPDH) transcripts was performed. Primers used for PCR amplification are listed in Table 2. The specific amplification of each gene transcript was confirmed by sequencing on an 8800 CEQ DNA sequencer (Beckman Coulter).

Immunoblotting. Kidneys from *CLDN16*$^{+/+}$ and *CLDN16*$^{-/-}$ animals were homogenized with a Polytron mixer (Kinematica, Lucerne, Switzerland) in 250 mM sucrose, 30 mM histidine, 1 mM EDTA (pH 7.4), 3 μg/ml leupeptine, 3 μg/ml pepstatine A, and 5 μg/ml aprotinin. After centrifugation at 1,000 *g* for 5 minutes at 4°C, the supernatants were collected and centrifuged again at 47,000 *g* for 1 hour at 4°C. After centrifugation, the pellets were solubilized in 50 mM Tris/Cl (pH 7.4), 1mM EDTA, and 2% SDS. Protein concentration was determined by the method of Bradford with a protein assay kit (Bio-Rad Laboratories, Hercules, CA, USA) using bovine serum albumin as the standard.

Aliquots of 7 μg of protein were separated by SDS- PAGE, and transferred onto

polyvinylidene difluoride filter (Millipore). The filters were incubated with anti-claudin antibodies, anti-ZO-1 pAb, or anti-β-actin mAb followed by incubation with anti-rabbit IgG (Dako) or anti-mouse IgG (Bio-Rad) antibody conjugated with horseradish peroxidase and the reacted polypeptides were visualized with the ECL chemiluminescence detection system (Amersham Biosciences).

Histochemical analysis

After fixation in 4% paraformaldehyde, kidneys were embedded in paraffin, and 3 μm-thick sections were prepared and stained with hematoxylin and eosin. The numbers of glomeruli in non-overlapping areas were counted in at least 10 fields of each fetal kidney section under the low-power field (x 100 magnification) microscopy.

Immunofluorescence microscopy

Serial 7μm frozen sections were prepared and were fixed in 95% ethanol at 4°C for 30 minutes, then in 100% acetone at room temperature for 1 min for detection of tight junction proteins, and in 100% acetone at -20°C for 20 minutes for THP staining. The sections were blocked with 1% bovine serum albumin in PBS for 20 minutes. One of the paired sections was incubated with anti-claudin-16 pAb and anti-occludin mAb for 30 minutes at ambient temperature, then washed three times in PBS, followed by incubation with secondary antibodies conjugated with AlexaFluor 488 conjugated or AlexaFluor 568 (Molecular Probes, Inc.). The other section was incubated with anti-THP pAb, followed by incubation with the secondary antibody conjugated with AlexaFluor 488. After washing with PBS, sections were embedded in ProLong antifade reagent (Molecular Probes, Inc.) and were examined with a Zeiss LSM 5 PASCAL

confocal laser-scanning microscope (Carl Zeiss). In some experiments, one of the sections was incubated with anti-claudin-3, -10, or -16 pAb and anti-claudin-4 mAb.

RESULTS

Expression of claudin-16 and other tight junction proteins in the kidneys from CLDN16$^{+/+}$ and CLDN16$^{-/-}$ animals

In the present study, we obtained fetuses homozygous for the deletion mutation of the *CLDN16* gene at different embryonic stages by embryo transfer technique. Since the full term in cattle is about day 280 of pregnancy, renal tissues from the P2 *CLDN16*$^{+/+}$ neonate was employed as the control for E270 *CLDN16*$^{-/-}$ fetus. The genotypes of these claudin-16-null fetuses and other animals examined were confirmed by a PCR-based typing of their genomic DNAs (Fig. 6A).

We first examined the expression of claudin-16 and some other claudins, which had been reported to be present in murine renal tubules [14], in the kidneys of *CLDN16*$^{+/+}$ and *CLDN16*$^{-/-}$ cattle at different ages. The RT-PCR analysis demonstrated that the expression of bovine claudin-16 RNA occurred in the kidney from *CLDN16*$^{+/+}$ E100 fetus and the neonate (P2) at the levels relevant to those in the normal 7-month-old (Fig. 6B). By contrast and as expected, no RT-PCR product for claudin-16 was detected in the kidney from *CLDN16*$^{-/-}$ fetuses and a 7-month-old animal (Fig. 6B). Unfortunately, immunoblotting of the renal crude membrane fractions failed to detect cluadin-16, presumably because of its low abundance (Fig. 6C).

RT-PCR and immunoblotting analyses demonstrated that, basically, there were no remarkable differences between *CLDN16*$^{+/+}$ and *CLDN16*$^{-/-}$ animals in the expression of other claudin subtypes, occludin, and ZO-1, although some samples exhibited low abundance of specific polypeptide examined (Figs. 6B and 6C). Low levels of expression of caludin-11 RNA demonstrated in the P2 neonate and 7-month-old animals,

compared with fetuses, were consistent with our observation on murine embryos (see Chapter III) and were not the subjects relevant to the presence or the absence of the claudin-16 expression.

Immunofluorescence analysis for the kidney of *CLDN16*$^{+/+}$ E100 fetus showed that claudin-16 was present and localized at the apicalmost regions of some renal tubules where fluorescent signals of occludin were also present (Fig. 7, upper panels). The distribution of claudin-16 in the *CLDN16*$^{+/+}$ E100 kidney was comparable with and restricted to that of the tubules positive for THP, a marker for the TAL segment, in the corresponding serial section, demonstrating a restricted expression of claudin-16 in the TAL segment as previously reported [14, 15] and as shown in Chapter I. In contrast, the THP-positive tubules in kidneys from *CLDN16*$^{-/-}$ E100 fetus had signals for occludin but gave no immunofluorescent signals for claudin-16 (Fig. 7, lower panels).

Renal morphology of claudin-16 deficient fetus

Figure 8 shows renal tissue sections, stained with hematoxylin-eosin, from *CLDN16*$^{+/+}$ and *CLDN16*$^{-/-}$ fetuses or neonate. There were no obvious abnormalities in the morphology of the renal tubules and glomeruli in the kidneys from *CLDN16*$^{-/-}$ fetuses (Figs. 8A-8F) compared with those from the *CLDN16*$^{+/+}$ wild-type controls (Figs. 8G-8I), throughout the fetal stage. Occasionally, in very limited areas, formation of a few small cysts (Figs. 8J and 8K) and rather mild mononuclear cell infiltrations (Figs. 8L and 8M) were observed only in the kidney from E270 *CLDN16*$^{-/-}$ fetus. Although the numbers of cortical glomeruli in the *CLDN16*$^{-/-}$ fetuses were slightly higher than those in normal fetuses at corresponding days of pregnancy, no statistic significance was obtained (Fig. 8N).

Expression and subcellular distribution of claudins expressed in the TAL of Henle's loop of CLDN16$^{-/-}$ kidneys

Our previous studies showed that, among the claudin subtypes examined involving claudins 1-4, 10, and 11, claudins 3, 4, and 10 were co-localized with claudin-16 at the TJ regions in the TAL segment of Henle's loop in nephrons of normal adult bovine kidneys (Chapter I). The expression of these claudins were examined in the kidneys of *CLDN16*$^{-/-}$ and *CLDN16*$^{+/+}$ fetuses and neonate, and found that their expression and subcelluar localization were basically the same with each other throughout the renal development. Figure 9 shows the representative expression patterns of claudin-3, -4, and -10 in the kidneys of E270 *CLDN16*$^{-/-}$ fetus and *CLDN16*$^{+/+}$ neonate. In the TAL of *CLDN16*$^{+/+}$ P2 neonate, claudin-4 was found co-localized with claudin-16 at the apicalmost region of the epithelial cell membranes, although prominent signals for claudin-4 were also found at the basolateral areas (Fig. 9A). Likewise, co-localization of claudin-3 and -10 with claudin-4 at the TJ region of renal tubules positive for THP were also shown in immunofluorescence microscopy (Figs. 9B and 9C), demonstrating the integrity of claudins 3, 4, 10, and 16 at the TJ of the TAL segment. All of these immunofluorescent signals, including basolateral signals for claudin-4, disappeared when the appropriate recombinant proteins containing the antigenic C-terminal region of each claudin were added to the immunostaining reactions. The *CLDN16*$^{-/-}$ E270 fetal kidney also showed co-localization of claudin-3 and claudin-10 with claudin-4 at the TJ regions of the tubules positive for THP (Figs. 9D and 9E), as observed in the kidney of wild-type P2 neonate, indicating that claudins 3, 4, and 10 are normally expressed in the TAL segment of developing renal tubules in *CLDN16*$^{-/-}$ fetuses. Basically, similar results

were obtained for the kidneys from *CLDN16*$^{-/-}$ and *CLDN16*$^{+/+}$ fetuses at different fetal stages (data not shown).

The integrated localization of claudins 3, 4, and 10 at the TJ of TAL segments were also obtained for both the 7-month-old *CLDN16*$^{-/-}$ animal and an age-matched *CLDN16*$^{+/+}$ animal (Figs. 10A-10E). Although the *CLDN16*$^{-/-}$ animal at 7 months of age exhibited aberrant renal lesions so that some THP-positive tubules had enlarged lumens, as typically seen in Fig. 10E, these tubules still remained distributions of these claudin subtypes at the TJs (Figs. 10D and 10E).

Table 2. Primers used for RT-PCR analysis of TJ protein mRNAs

Sequences of the primer pairs for PCR amplification of claudins, occludin, ZO-1, and GAPDH cDNAs and the GenBank accession numbers for the genes or clones containing the primer sequences are presented.

Proteins	Sequence	Accession number
Claudin-1	Forward, 5'-GGCTATTTTAGTTGCCACAGC-3'	AB178476
	Reverse, 5'-ACACATAGTCTTTCCCACTGG-3'	
Claudin-2	Forward, 5'-CCTGGGCTTCATTCCTGTTGC-3'	AB115779
	Reverse, 5'-CTCACTCTTGCCTTTCGGCGC-3'	
Claudin-3	Forward, 5'-TCCTGCCCGCCGCGCGACAAC-3'	AB115781
	Reverse, 5'-CCATCAGACGTAGTCCTTGCGGTC-3'	
Claudin-4	Forward, 5'-GGATCCTCAGCGCCTTTTCAG-3'	AB185928
	Reverse, 5'-CCAAGGATCAGCAAGCCAGCG-3'	
Claudin-10	Forward, 5'-GGCATGGCGAGCACGG-3'	BT020910
	Reverse, 5'- CACAGCTTGAAGGCAGCTCTC-3'	
Claudin-11	Forward, 5'-CGGCTATTCTCCTGCTGCTCAC-3'	XM_585024
	Reverse, 5'-GGCAGAGGAGTGGGCTTCCCA-3'	
Claudin-16	Forward, 5'-CTGGAGGTGAGCACAAAATGC-3'	AB030082
	Reverse, 5'-ACCCAAAGAACCAGCCATTCC-3'	
Occludin	Forward, 5'-GACTGGATCAGGGAATATCCACC-3'	XM_590937
	Reverse, 5'-AGCAGCAGCCATGTACTCTTCAC-3'	
ZO-1	Forward, 5'-CAAAGAAGGCTTGGAGGAGGG-3'	AJ313183
	Reverse, 5'-TCCATAGGGAGATTCCTTCTC-3'	
GAPDH	Forward, 5'-ATCGGGCGCCTGGTCACCAGGGCT-3'	AJ000039
	Reverse, 5'-GAAGACCCCAGTGGACTCCACTACATA-3'	

A

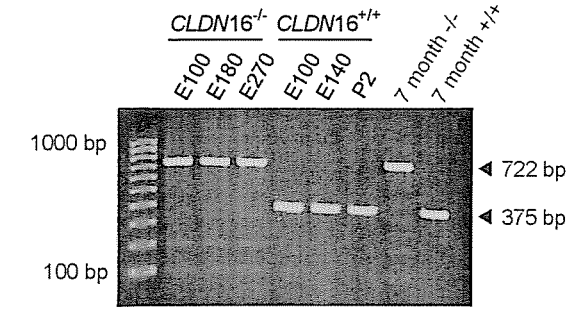
CLDN16-/-
CLDN16+/+
E100
E180
E270
E100
E140
P2
7 month -/-
7 month +/+
1000 bp
100 bp
722 bp
375 bp

B

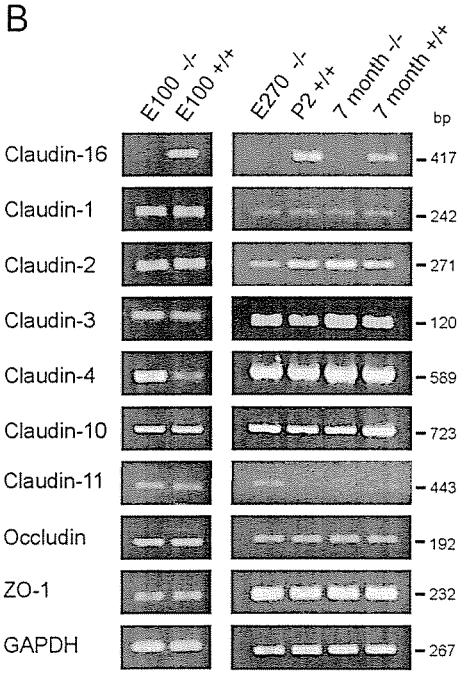
E100 -/-
E100 +/+
E270 -/-
P2 +/+
7 month -/-
7 month +/+
bp
Claudin-16
Claudin-1
Claudin-2
Claudin-3
Claudin-4
Claudin-10
Claudin-11
Occludin
ZO-1
GAPDH
417
242
271
120
589
723
443
192
232
267

C

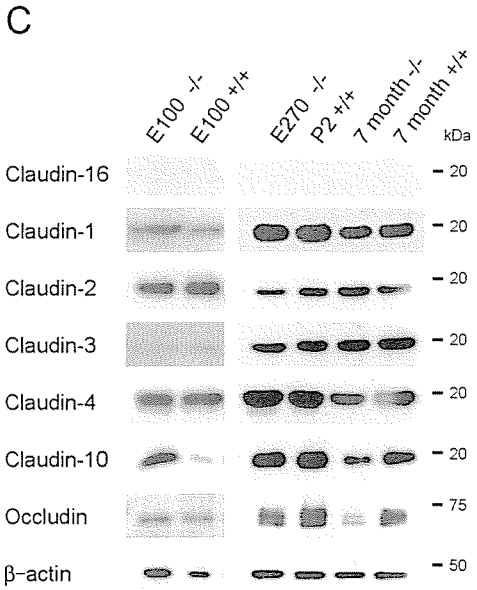
E100 -/-
E100 +/+
E270 -/-
P2 +/+
7 month -/-
7 month +/+
kDa
Claudin-16
Claudin-1
Claudin-2
Claudin-3
Claudin-4
Claudin-10
Occludin
β-actin
20
20
20
20
20
20
75
50

Fig. 6. Genotyping of the animals and expression of tight junction proteins in *CLDN16*$^{-/-}$ kidneys. (*A*) Genotyping for *CLDN16*. *CLDN16*$^{-/-}$ fetuses at embryonic day 100 (E100), 180 (E180) and 270 (E270) exhibited to possess the type-1 mutant allele in homozygous state representing 722-bp fragment in PCR, whereas age-matched normal *CLDN16*$^{+/+}$ animals gave 375-bp fragment. The fragments of PCR amplification from adult cattle homozygous for (+/+) or free from (-/-) type-1 *CLDN16* mutation are also shown. (*B*). RT-PCR analysis for the expression of mRNAs of claudins 16, 1-4, 10, and occludin, and ZO-1 in the kidneys from *CLDN16*$^{-/-}$ fetuses at E100 (*E100-/-*) and E270 (*E270-/-*), a 7-month-old *CLDN16*$^{-/-}$ animal (*7 month -/-*), E100 *CLDN16*$^{+/+}$ fetus (*E100+/+*), a *CLDN16*$^{+/+}$ neonate (*P2+/+*), and a 7-month-old cattle (*7 month +/+*). Representative results of three separate experiments are shown. The expression of glyceraldehyde 3-phosphate dehydrogenase (*GAPDH*) is included as the control. The sizes of PCR products are indicated in bp. (*C*) Immunoblotting analyses for claudins 16, 1-4, and 10) and occludin in crude membranes from kidneys of the animals. β-Actin was used as the control for protein loading.

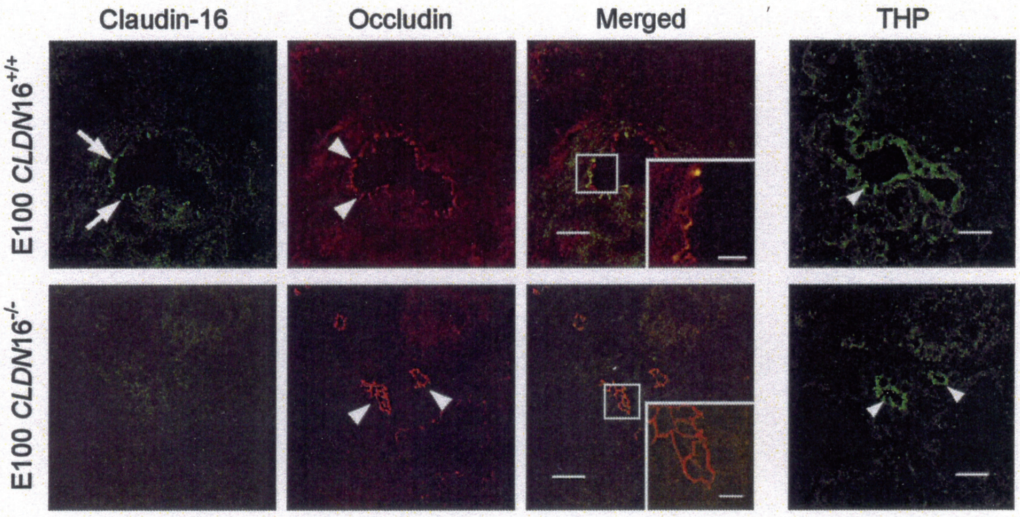

Figure 7. Immunofluorescent detection of claudin-16 in E100 *CLDN16*$^{+/+}$ and *CLDN16*$^{-/-}$ fetuses. One of the frozen sections of the kidney from *CLDN16*$^{+/+}$ or *CLDN16*$^{-/-}$ E100 fetus was reacted with the anti-THP pAb (right panels). Small arrowheads indicate the signals specific to THP. The other one was double-stained with the anti-claudin-16 pAb and anti-occludin mAb (left panels). Arrows and arrowheads indicate the signals specific to claudin-16 and occludin, respectively. Merged image for the *CLDN16*$^{+/+}$ fetus indicates co-localization of claudin-16 and occludin at the apicalmost region of the cells in THP-positive renal tubules. The inserted images are the magnifications of the outlined areas. Bars = 20 μm and 5 μm in the inserted figures.

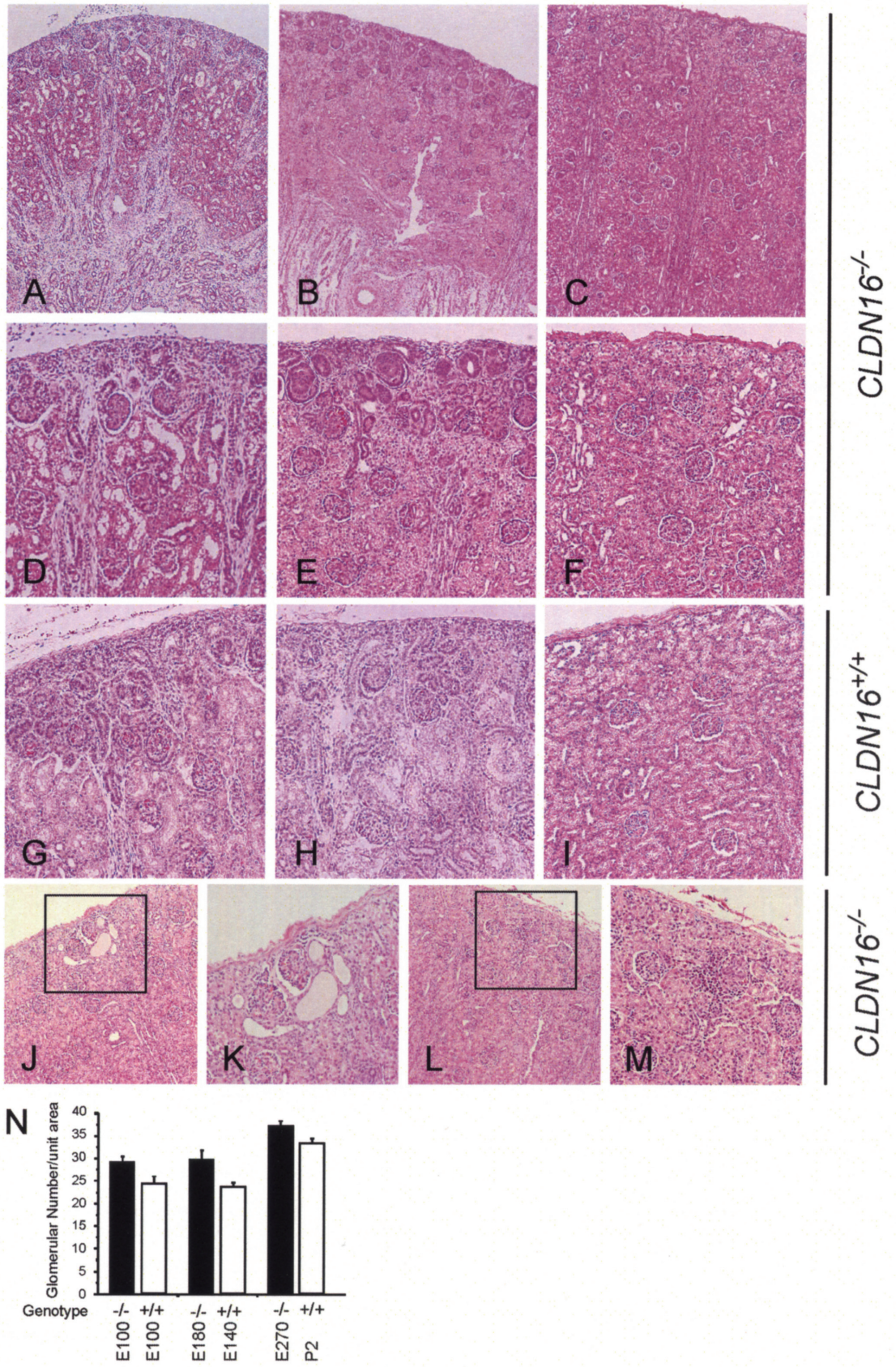
A
B
C
D
E
F
G
H
I
J
K
L
M
CLDN16-/-
CLDN16+/+
CLDN16-/-
N
Glomerular Number/unit area
40
35
30
25
20
15
10
5
0
Genotype
-/- +/+ -/- +/+ -/- +/+
E100 E100 E180 E140 E270 P2

Figure 8. Renal morphology of *CLDN16*$^{-/-}$ and *CLDN16*$^{+/+}$ fetuses. *A-F*, low-power views (*A-C*) and high-power views (*D-F*) of the kidneys of *CLDN16*$^{-/-}$ fetuses at E100 (*A* and *D*), E180 (*B* and *E*), and E270 (*C* and *F*). None of them shows no obvious morphological abnormality. *G-I*, high-power views of the kidneys of *CLDN16*$^{+/+}$ fetuses at E100 (*G*), E140 (*H*), and that of postpartum day 2 neonate (P2) (*I*). *J-M*, minimal pathological changes found in the *CLDN16*$^{-/-}$ E270 fetus. Cyst formation (*J* and *K*) and mononuclear cell infiltration (*L* and *M*) were occasionally observed in limited areas of the kidney of *CLDN16*$^{-/-}$ E270 fetus. *N*, cortical glomerular numbers in *CLDN16*$^{-/-}$ fetuses (▯) and age-matched *CLDN16*$^{+/+}$ control (▯) were counted for each filed under low-power microscopy and are presented as the mean ± S.D. (n = 10). *O* and *P*, immunohistochemical localization of PCNA-positive cells (arrows) in the kidneys of *CLDN16*$^{-/-}$ E270 fetus (*O*) and P2 neonate (*P*). Original magnifications were x 40 for *A-C*, x 100 for *D-J* and *L*, and x 200 for *K* and *M*.

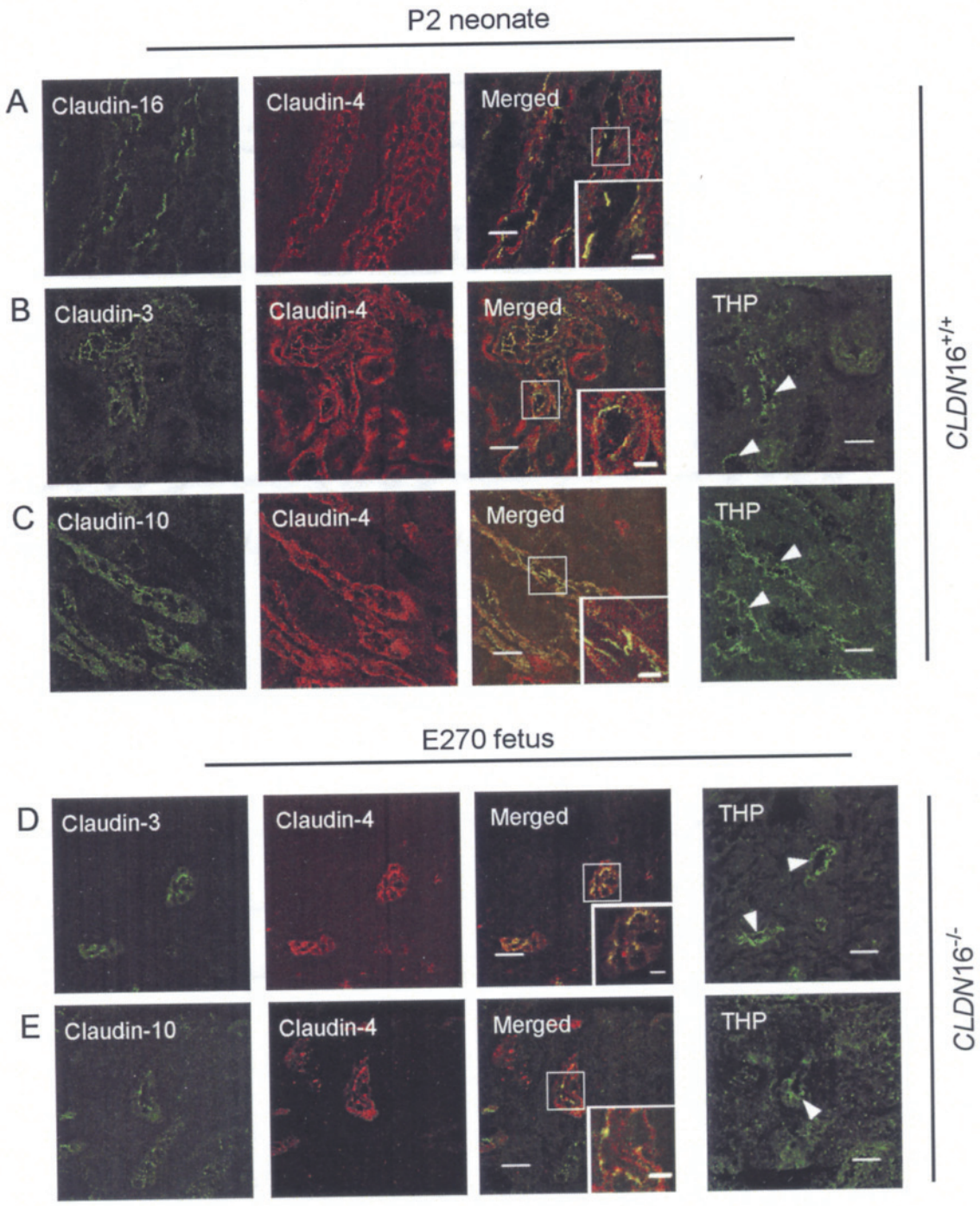
P2 neonate
A
Claudin-16
Claudin-4
Merged
B
Claudin-3
Claudin-4
Merged
THP
C
Claudin-10
Claudin-4
Merged
THP
CLDN16+/+
E270 fetus
D
Claudin-3
Claudin-4
Merged
THP
E
Claudin-10
Claudin-4
Merged
THP
CLDN16-/-

Figure 9. Localization of claudins 16, 3, 4, and 10 in the TAL segments of P2 *CLDN16*$^{+/+}$ neonate and E270 *CLDN16*$^{-/-}$ fetus. One of the paired frozen sections from P2 *CLDN16*$^{+/+}$ neonate (*A-C*) and E270 *CLDN16*$^{-/-}$ fetal kidneys (*D* and *E*) were double-stained with appropriate anti-claudin pAb and anti-claudin-4 mAb and their images are overlayed (Merged). The other section was stained for THP to examine the presence of claudins other than claudin-16 in the tubules positive for THP in the corresponding paired section (right panels). Arrowheads indicate the signals specific to THP. The inserted figures are the magnified images of outlined regions in the overlays. Bars = 5 μm for the inserted images and 20 μm for others.

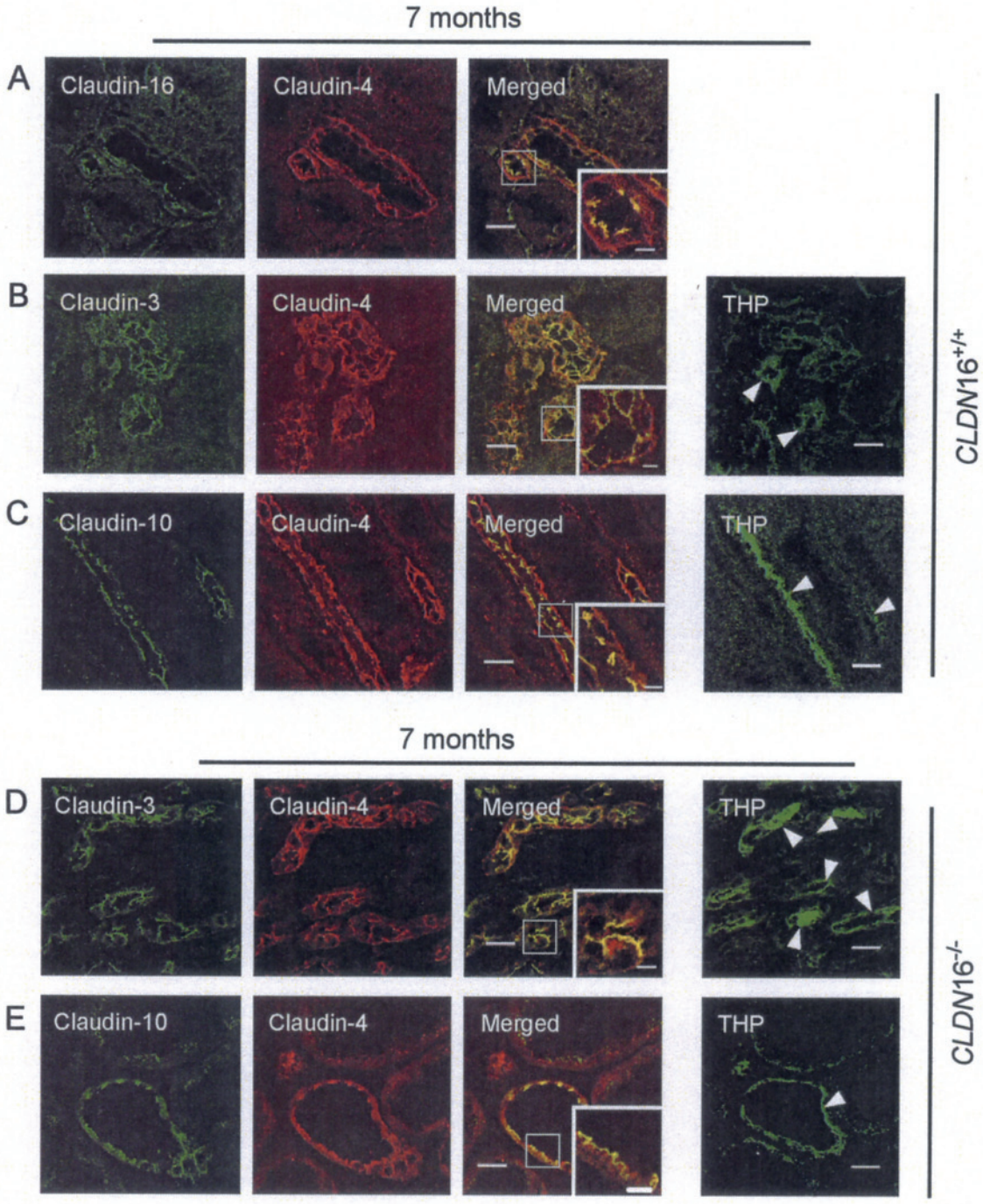

Figure 10. Localization of claudins 16, 3, 4, and 10 in the TAL segments of 7-month-old *CLDN16*$^{+/+}$ and *CLDN16*$^{-/-}$ animals. The paired renal frozen sections from 7-month-old *CLDN16*$^{+/+}$ (*A-C*) and *CLDN16*$^{-/-}$ (*D* and *E*) animals were processed for detection of claudin proteins and THP, and are presented as described in the legend for Fig. 4.

DISCUSSION

Renal pathology of bovine claudin-16 deficiency is characterized by tubular dyspalsia associated with the presence of immature tubular epithelia and interstitial fibrosis that are found even in one-to two-month-old calves [22], suggesting that the renal lesions appear during the prenatal development of the kidney. However, the findings of the present study demonstrated that the kidneys of the *CLDN16*$^{-/-}$ animals exhibited normal morphological development of nephrons during the prenatal stage without aberrant lesions (Fig. 8), indicating that the presence of claudin-16 itself is not critical to the process in development and formation of renal tubules. Our data also showed that the lack of claudin-16 caused no obvious change in distribution of other claudin subtypes, claudin-3, -4, and -10, at the TJ in the TAL segment (Figs. 9 and 10). These findings indicate that one or some of claudins 3, 4, and 10 are enough to form the principal structure of TJs required for cell-cell adhesion in the TAL region. This is supported by the observation that each of these claudins can form TJ-like structures to adhere to each other between adjacent cells when transfected into fibroblast cell line L cells [25], although it does not rule out the possibility that claudin-16 strengthens the cell-cell adhesion in normal epithelia. In addition, several reports on the mice with disruption of the *Cldn5* [43] and *Cldn1* [44] genes have shown the similar observations. In *Cldn5*-null mice, removal of claudin-5 from the TJs in the brain vessels, consisting of claudin-5 and -12, caused size-selective loosening of the blood brain barrier, but did not alter morphology of blood vessels and formation of TJs of endothelial cells [43]. The *Cldn1*-null mice failed to maintain the epidermal permeability barrier, whereas TJ strands of epidermis, containing claudin-4 as well as claudin-1, were not affected

morphologically [44]. Thus, it is likely that some of multiple claudins consisting of TJ strands in certain tissues are indispensable in the specific barrier function, but are redundant in formation of the tissues. In contrast, *Cldn11*-deficient mice demonstrated neurological and reproductive deficits due to the absence of TJs in the central nervous system myelin and between Sertoli cells [45], suggesting that claudin-11 is either the only claudin molecules in these TJs, or that it is essential for TJ formation and maintenance.

The formation of morphologically normal renal tubules in *CLDN16*$^{-/-}$ fetuses also indicates that the development of renal lesions has the onset in the early stage of neonatal periods. This coincides with the formation of small cysts and slight infiltration that were occasionally observed in E270 *CLDN16*$^{-/-}$ fetus with nearly full term of pregnancy (Fig. 8). The morphological abnormality appears to be developed by at most one month after birth [22] and progressively lead to aberrant tubular atrophy [22, 41]. Hence, the major causes for renal lesions in bovine claudin-16 deficiency likely involve dysfunction of the TJ at TAL segments in regulating the paracellular permeability, disabling the maintenance of the tubules.

Interestingly, *Cldn14*-null mice demonstrated deafness with postnatal onset due to cochlear outer hair cell degeneration, although TJ strands at this region were still present and appeared morphologically normal [46]. Altered ionic permeability of the paracellular barrier of the reticular lamina due to the absence of claudin-14 has been suspected to cause prolonged depolarization and eventual death of outer hair cells leading to deafness [46]. A recent study by Hou *et al.* [47] has shown that human claudin-16/paracellin-1 modulates the ion selectivity of the TJ to remarkably increase the permeability of Na^+ without significant effect on Cl^- in transfected LLC-PK1 cells,

and suggested that claudin-16/paracellin-1 regulates the level of transepithelial voltage as the primary driving force for Mg^{2+} and Ca^{2+} reabsorption in TAL epithelia [48]. They also showed that the amino acid sequence in the first extracellular loop was critical for the Na^{+}-selective permeability of claudin-16/paracellin-1 [47]. Since the amino acid sequence in the corresponding region of bovine claudin-16 is highly homologous to that in the human counterpart, *i. e.*, only a single amino acid residue in this region consisting of 56 amino acid residues is different between bovine and human claudin-16, it is not unreasonable to suspect that bovine caludin-16 has a similar ion selectivity to generate transepithelial potential for passive paracellular flow of Mg^{2+} and Ca^{2+}. Thus, the lack of claudin-16 in the TAL segments in the bovine kidney would lead to the loss of the lumen-positive potential and subsequent reduction in reabsorption of divalent cations, as has been suggested for FHHNC [47].

Moreover, in contrast to the supposed role of claudin-16 in paracellular transport of Na^{+}, claudin-4 selectively decreases the permeability of Na^{+} [40]. Therefore, the presence of claudin-4, in addition to the lack of claudin-16, in TAL segments of affected animals could greatly enhance the transcellular concentration gradient of NaCl from peritubular space to the lumen compared to that formed under normal conditions. This may cause some metabolic changes in TAL epithelial cells, as suggested for cochlear hair cell degeneration in claudin-14 deficiency [46], leading to consequent cellular death and development of renal tubular dysplasia. In addition, even under physiological conditions, the coexistence of claudin-4 seems to affect the claudin-16 function in generating the lumen-positive potential in the TAL segments of bovine nephrons, suggesting that reabsorption of divalent cations in TAL regions is less fundamental in cattle. This may partly explain why the affected animals do not have aberrant

phenotypes in Mg^{2+} and Ca^{2+} metabolisms [24].

However, the roles of claudin-16 in paracellular transport and the mechanisms for it are still obscure. Although Hou *et al.* [47] reported increased permeability of Na^{+} in LLC-PK1 cells transfected with claudin-16, they found no significant effect of claudin-16 on paracellular permeabilities of Na^{+}, Cl^{-}, and Mg^{2+} in MDCK II cells. In contrast, Ikari *et al.* [49] reported that rat claudin-16 increased transepithelial electrical resistance, representing decreased ion permeability, and apical to basal paracellular transport of $^{45}Ca^{2+}$ in a manner dependent of the electrical potential gradient in transfected MDCK II cells. Furthermore, our preliminary study using MDCK I cells showed that expression of bovine claudin-16 caused reduction of paracellular transport of $^{45}Ca^{2+}$ in both from apical to basal and from basal to apical directions (H. Ohta, H. Adachi, S. Shibutani, K. Ono, and M. Inaba, unpublished observation). These discrepancies may be partly explained by a model in which exogenous claudins add new charge-selective pores leading to a physiological phenotype that combines contributions of both endogenous and exogenous claudins in the cells. The physiological role and the regulatory mechanism for functional interaction of claudin-16 and claudin-4, and claudins 3 and 10 as well, in cattle remain to be investigated.

The pathogenesis for inflammatory lesions in claudin-16 deficiency also remains unknown. Epithelial cells in TAL segments produce THP and secret it into urine [50, 51]. THP is a powerful autoantigen and is involved in several forms of inflammatory kidney diseases [50, 51] including deposition of immune complex containing THP and the antibody in the intercellular space of the TAL region [52-54]. Therefore the barrier function of TJs in the TAL appears to be important to segregate the protein from the immune system. Disruption of TAL epithelial cells due to claudin-16 deficiency would

lead to leakage of THP into peritubular space, and may cause inflammatory response and subsequent renal damage.

In conclusion, this study demonstrated that the absence of claudin-16 in the TJs at TAL of Henle's loop in bovine kidneys did not affect morphologically the renal tubular formation during prenatal stage *in utero*. Bovine claudin-16 appears to be indispensable for its selective paracellular permeability required for the maintenance of renal tubular architectures.

SUMMARY

Claudin-16 deficiency in cattle due to the deletion mutations of the *CLDN16* gene results in renal tubular dysplasia, interstitial nephritis, and severe renal failure of affected animals at their neonatal stage, suggesting that the total lack of a tight junction protein claudin-16 affects tubular formation in the fetal period as well as dysfunction of paracellular transport. To examine the prenatal pathogenesis in the claudin-16 deficiency, $CLDN16^{-/-}$ bovine fetuses at embryonic days 100, 180, and 270 were generated by embryo transfer. Tubular formation was studied histologically and the expression of the tight junction proteins, including claudins 16, 1-4, 10, and 11, and occludin, were examined. $CLDN16^{-/-}$ fetuses showed no histological abnormality compared with normal $CLDN16^{+/+}$ fetuses even at 270 days of gestation. Claudins 3, 4, and 10 were constitutively distributed at the tight junction of the renal tubular segment positive for Tamm-Horsfall glycoprotein, the thick ascending limb of Henle's loop, where claudin-16 was exclusively distributed, in the kidneys of $CLDN16^{-/-}$ fetuses as in normal $CLDN16^{+/+}$ kidneys. Distributions of claudins 3, 4, and 10 were also found at the thick ascending limb regions in the kidney with tubular dysplasia from a 7-month-old $CLDN16^{-/-}$ animal. These findings demonstrate that deficiency of claudin-16 did not cause apparent morphological abnormality in renal tubules during the period of renal development *in utero*. Thus, claudin-16 appears necessary for the maintenance of normal tubular architecture after birth presumably by its function of paracellular transport mechanism.

CHAPTER III

Developmental changes in the expression of tight junction protein claudins in murine metanephroi and embryonic kidneys: a model for studies on claudin-16 function

INTRODUCTION

The claudins are a family of more than 20 homologous subtypes which share the same membrane topology and have various tissue-specific and segment-specific distribution patterns [3, 27]. Heterogenous claudins form individual TJ strands as heteropolymers to adhere to each other at the cell-cell interface [25] to generate consequential variations in the tightness of individual TJ strands [27].

Pathological phenotypes of humans and animals with mutations in genes of specific claudins, including claudins 11 [45], 14 [46, 55], and 16 [15, 19, 20], demonstrate the importance of these TJ proteins in the formation and maintenance of epithelial architecture. However, the precise mechanisms for degeneration of cells and tissues in these diseases, including claudin-16 deficiency in cattle, remain unknown.

To examine physiological and pathological roles of claudin-16, experimental systems in which expression of specific claudin genes can be regulated are desirable. Expression of various claudins in monolayers of several cell lines, including MDCK and LLC-PKI cells, has been employed to characterize their barrier functions [38, 40, 47, 49]. However, there is a limitation of this type of approach as discussed in Chapter II. Organotypic culture of metanephric explants seem to be an adequate model for this purpose since various studies have shown that mouse metanephroi removed from embryos continue to develop *in vitro* and display many of the processes of nephron induction and differentiation that are observed *in vivo* [56-58] and the expression of specific genes can be inhibited in the presence of antisense oligonucleotides [59] and/or interfering RNAs [60]. In the present study, we examined the expression of several different claudin genes in metanephroi and compared them with those in embryos to

elucidate if metanehroi actually have normal expression levels and patterns for the claudins.

MATERIALS AND METHODS

Antibodies

Antibodies used in this Chapter were described in Chapter I.

Animals

Pregnant ICR mice purchased from Japan SLC (Hamamatsu, Japan) were housed in our own animal facility under conventional conditions, and the appearance of a vaginal plug was designated as day 0 of gestation. All experimental procedures met with the approval of the Laboratory Animal Experimentation Committee, Gaduate School of Veterinary Medicine, Hokkaido University.

Developmental analysis of the tight junction proteins in mouse embryonic kidneys

Embryos were removed from anesthetized pregnant ICR mice on embryonic days (E) 12, 14, 16, and 18 of the pregnancy and were dissected to obtain metanephoi. Total RNAs were prepared, reverse-transcribed into cDNAs as described previously [61], and amplified by PCR for claudins 1-4, 8, 10, 11, and 16, occludin, ZO-1, and glyceraldehyde 3-phosphate dehydrogenase. The amplified cDNA fragments were confirmed by sequencing on a CEQ8800 DNA analysis system (Beckman Coulter). Primers used for PCR amplification are listed in Table 3.

Organ cultures

Metanephroi culture was carried out essentially as described previously[58, 59]. Metanephroi isolated from E12 embryos were placed on a Millicell®-CM cell culture plate insert (Millipore, Bedford, MA, USA) and cultured. A 25-mm diameter organ

culture insert allowed placement of a minimum of six metanephroi in an interface in the presence of medium consisting of a 1:1 mixture of Dulbecco's modified Eagle's medium and F12 supplemented with 10% fetal bovine serum FBS and a 5-fold concentration of MITO serum extender (BD Biosciences, Bedford, MA, USA).

Cultured metanephroi were frozen in liquid nitrogen with or without OCT compound (Sakura Fine Technical Co.) for immunohistochemistry and RNA analyses, respectively. Total RNAs were prepared from cultured metanephroi using an RNeasy Micro kit (QIAGEN GmbH, Hilden, Germany) and reverse-transcribed into cDNAs for RT-PCR analysis as described above. Cryostat sections of cultured metanephroi were prepared for histological and immunohistochemical analyses. Cryostat sections of post-explant day 2 (p.e.2), p.e.4, p.e.6, and p.e.8 metanephroi were fixed in 10% neutral buffered formalin and stained with hematoxylin and eosin.

Immunofluorescence microscopy

Cryostat sections of p.e.8 metanephroi were fixed with 95% ethanol at 4°C for 30 minutes, followed by 100% acetone at room temperature for 1 minute. Sections were incubated with 1% bovine serum albumin in PBS for 20 minutes. Sections were then incubated with the appropriate anti-claudin antibodies and the anti-occludin or anti-ZO-1 antibody. Sections were then washed three times with PBS, followed by incubation for 30 minutes with secondary antibodies conjugated with AlexaFluor 488 or 568 (Molecular Probes, Inc.). After washing with PBS, sections were embedded in Prolong antifade reagent (Molecular Probes, Inc.) and examined under an ECLIPSE E800 microscope equipped with a deconvolution apparatus (Nikon, Tokyo, Japan).

The specificities of immunofluorescent signals for some claudins, including

claudins 1-4 and 16 were examined using the GST-tagged recombinant proteins (Chapter I). Immunofluorescent signals with these antibodies in mouse kidney sections disappeared when each GST-fused protein was included in the reaction (data not shown), indicating that the antibodies to claudins 1-4 and 16 used in this study immunospecifically recognized each claudin from cattle and mice. In addition, anti-claudin-8 and anti-claudin-10 antibodies, both raised against their C-terminal peptide regions, did not react with GST fusion proteins described above in immunoblotting (data not shown).

While we could identify renal tubular segments in the kidney from adult mice using the antibodies to several segment-specific marker proteins as reported by previous investigators [14], frozen sections of p.e.8 metanephroi showed no or very faint staining for some of these markers including the Tamm-Horsfall glycoprotein, a marker of the TAL segment. Thus, we have not defined the specific tubular segments in developing metanephroi in the present study.

RESULTS

Expression of claudins, occludin, and ZO-1 in mouse embryonic kidneys

We first examined the expression of claudins, occludin and ZO-1 in mouse developing kidneys by RT-PCR. Constant expression of ZO-1, a peripheral membrane protein, was detected throughout the period examined. Likewise, claudins 1, 3, 4, 8, and 11, and occludin as well, were observed in the metanephroi at E12, and most of them reached increased levels afterward till E18, corresponding to the levels in the adult kidney (Fig. 11A). The only exception was claudin-11, which presented a high level of expression throughout E12 to E18 and then appeared to be reduced to the low level observed in adult animals.

In contrast, signals for claudins 2, 10, and 16 were not obvious at E12, they appeared clear on E14 and then increased to the adult levels (Fig. 11A). Consistent with this observation, the immunofluorescent signals for claudin-16 were demonstrated as early as E15 at the apical end regions of adjacent epithelial cells and appeared abundant from E16 onward during in utero development (Fig. 11B).

Organ culture and in vitro expression of TJ proteins

Metanephroi from E12 embryos continued to grow in vitro till post-explant day 8 (p.e.8) and showed increases in tubular branching with formation of comma-shaped or S-shaped metanephric tubules (Figs. 12A and 12B), consistent with previous observations [56, 58]. Histological features of metanephroi shown in Fig. 12B were principally the same as those observed in embryonic kidneys at corresponding days after gestation (data not shown), indicating that the process of tubular development in

metanephroi represented that in developing kidneys in vivo as shown in previous studies [57, 58]. These metanephroi exhibited expression patterns of the TJ protein genes that were principally the same as those obtained for kidneys from embryos (Fig. 13A). PCR-amplified fragments of claudins 1, 3, 4, 8, 10, and 11 and ZO-1 were found throughout the incubation period. Apparent increases in signal intensities of claudin-1 and -10 and the expression of claudin-11 at high and constant levels during the incubation were comparable to those observed in embryonic kidneys (Fig. 11A). Moreover, the signals for claudin-16 and occludin were detected from p.e.2 onward (Fig. 13A). Occasionally, very weak but demonstrable signals were found for claudin-2 and -3 in metanephroi on the day of dissection, p.e.0 as shown in Fig. 13A, presumably due to low levels of expression of these claudins around E12.

Immunofluorescence microscopy of occludin and ZO-1 in the p.e. 8 metanephroi showed that these proteins principally colocalized at the apicalmost regions of lateral membranes in tubular epithelial cells, indicating the formation of TJ in these regions (Fig. 13B). Fluorescent signals for occludin in some individual tubular segments were not obvious as compared to signal intensities of ZO-1 in the corresponding areas, possibly reflecting low levels of the relative abundance of occludin.

Immunofluorescence microscopy also showed that various claudin species, including claudins 1-4, 8, 10, and 16, were present in the p.e.8 metanephroi (Fig. 13B). A series of combined images for the claudins and occludin, or ZO-1, demonstrated that the fluorescent signals for individual claudins were merged with some but not all of those for occludin and ZO-1 in the corresponding areas of the tissue sections. This indicated that these claudins were present at the TJ and that distribution of individual claudins was restricted to one or several specific tubular segments. Unfortunately,

however, we could not identify each tubule segment to distinguish the tubular localization of each claudin, because the tubules in the metanephroi, both grown in culture and in utero, lacked staining or had very weak and equivocal staining with several different markers specific to each segment such as the Tamm-Horsfall glycoprotein, which specifically discriminates the TAL from other tubular segments in adult kidneys (data not shown and ref. 14).

Table 3. Primers used for RT-PCR analysis of the TJ protein mRNAs

Sequences of the primer pairs for PCR amplification of claudins, occludin, ZO-1, and glyceraldehydes 3-phosphate dehydrogenase (GAPDH) cDNAs and the GenBank accession numbers for the genes or clones containing the primer sequences are presented.

Proteins	Sequence	Accession number
Claudin-1	Forward, 5'-GCATCCTGCTGGGGCTGATCG-3'	AF072127
	Reverse, 5'-GGCTTGGGATAAGGCCGTGGTG-3'	
Claudin-2	Forward, 5'-CGTCCAGTGCAATGTCCTCGCTG-3'	BC015252
	Reverse, 5'-AGCCACTACCCCACCCTACCC-3'	
Claudin-3	Forward, 5'-AGCCGGTTCAAGTCCAGCAGC-3'	NM_009902
	Reverse, 5'-CCTTGCGGTCGTAGGCGGTG-3'	
Claudin-4	Forward, 5'-AGCTGGTGCATCGGACTCAGC-3'	NM_009903
	Reverse, 5'-TCCCCAGCAAGCAGTTAGTGGC-3'	
Claudin-8	Forward, 5'-TGTGCTGCGTCCGTCTTGGC-3'	BC003868
	Reverse, 5'-CGGCGTGGAAACTCCGTTGAGTG-3'	
Claudin-10	Forward, 5'-CCGGTGTCGCCAACTGCAAG-3'	NM_021386
	Reverse, 5'-GTCCGAGAAGACATGACAGACGTGG-3'	
Claudin-11	Forward, 5'-CCGCCATCTTGCTGCTGTTGAC-3'	BC021659
	Reverse, 5'-GGCAGGGAAGTGGGCTTCTCC-3'	
Claudin-16	Forward, 5'-CCCATGTGTCCCTTCCCAACAGG-3'	NM_053241
	Reverse, 5'-GTCTCTGTCCGAGGGGCCTTG-3'	
Occludin	Forward, 5'-GACTGGGTCAGGGAATATCCACC-3'	NM_008756
	Reverse, 5'-AGCAGCAGCCATGTACTCTTCAC-3'	
ZO-1	Forward, 5'-CCACCAAGGTCACACTGGTG-3'	NM_009386
	Reverse, 5'-CGAGCGACCTGAATGGTCTG-3'	
GAPDH	Forward, 5'-GAAGGTCGGTGTGAACGGATT-3'	NM_008084
	Reverse, 5'-GAAGACACCAGTAGACTCCACGACATA-3'	

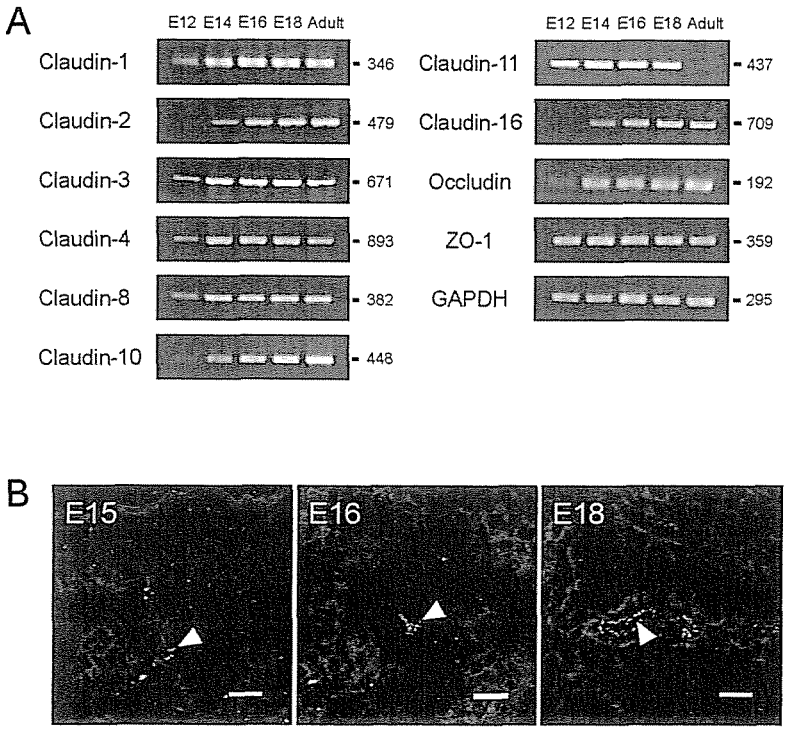

Figure 11. Expression of claudins, occludin, and ZO-1 in developing and adult mouse kidneys. *A*, the expression of mRNAs for claudins (claudins 1-4, 8, 10, 11, and 16), occludin, and ZO-1 in mouse embryonic kidneys at day 12, 14, 16, and 18 of gestation (E12-E18) and adult mouse kidneys (Adult) was analyzed by RT-PCR followed by electrophoresis on agarose gels and the representative results of two separate experiments are shown. The expression of glyceraldehyde 3-phosphate dehydrogenase (GAPDH) is included as a control. The sizes of PCR products are indicated in bp. *B*, immunofluorescent detection of claudin-16 in embryonic kidneys. Frozen sections of the kidneys from mouse embryos at E15, E16, and E18 were reacted with the anti-claudin-16 pAb followed by detection with a secondary antibody labeled with AlexaFluor 488 (arrowheads). Bars = 20 μm.

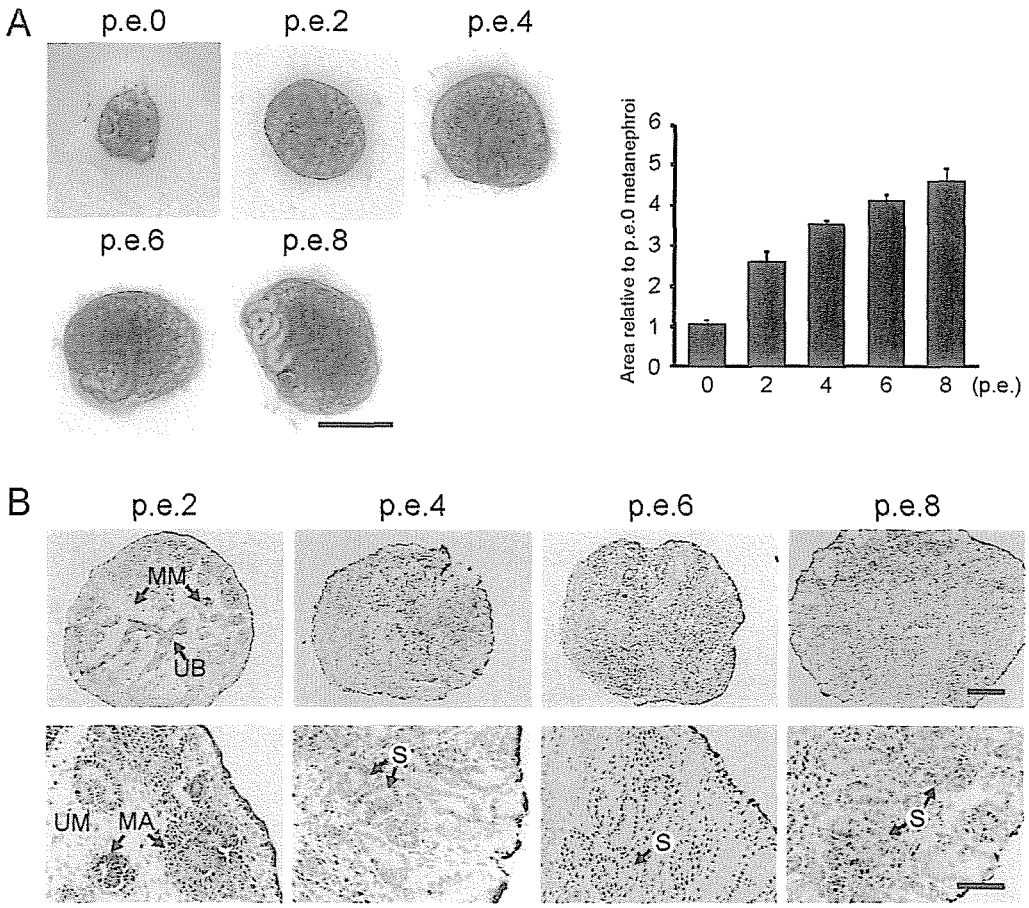

Figure 12. Growth of mouse metanephroi in culture. *A*, metanephroi isolated from E12 (= p.e.0) mouse embryos were cultured on membrane filters for 2 (p.e.2), 4 (p.e.4), 6 (p.e.6), and 8 (p.e.8) days and were photographed under a bright-field microscope (left). The mean sizes of metanephric explants at days p.e.0 through p.e.8 were estimated as the areas of the organs in photos using NIH Image software. The ratios of areas relative to those of p.e.0 metanephroi are presented as the mean ± S.D. (n = 6) (right). Bar = 1 mm. *B*, histological changes of cultured mentanephroi. Cryostat sections of cultured metanephroi stained with hematoxylin and eosin are presented with low-power views (upper panels, original magnification, x 40) and high-power views (lower panels, original magnification, x 200). The branched ureteric bud (UB), metanephric mesenchyme (MM), mesenchymal aggregates (MA), and uninduced mesenchyme (UM) are indicated with arrows. comma- and/or S-shaped metanephric tubules (S) are also indicated. Bars = 200 μm (upper panels) and 50 μm (lower panels).

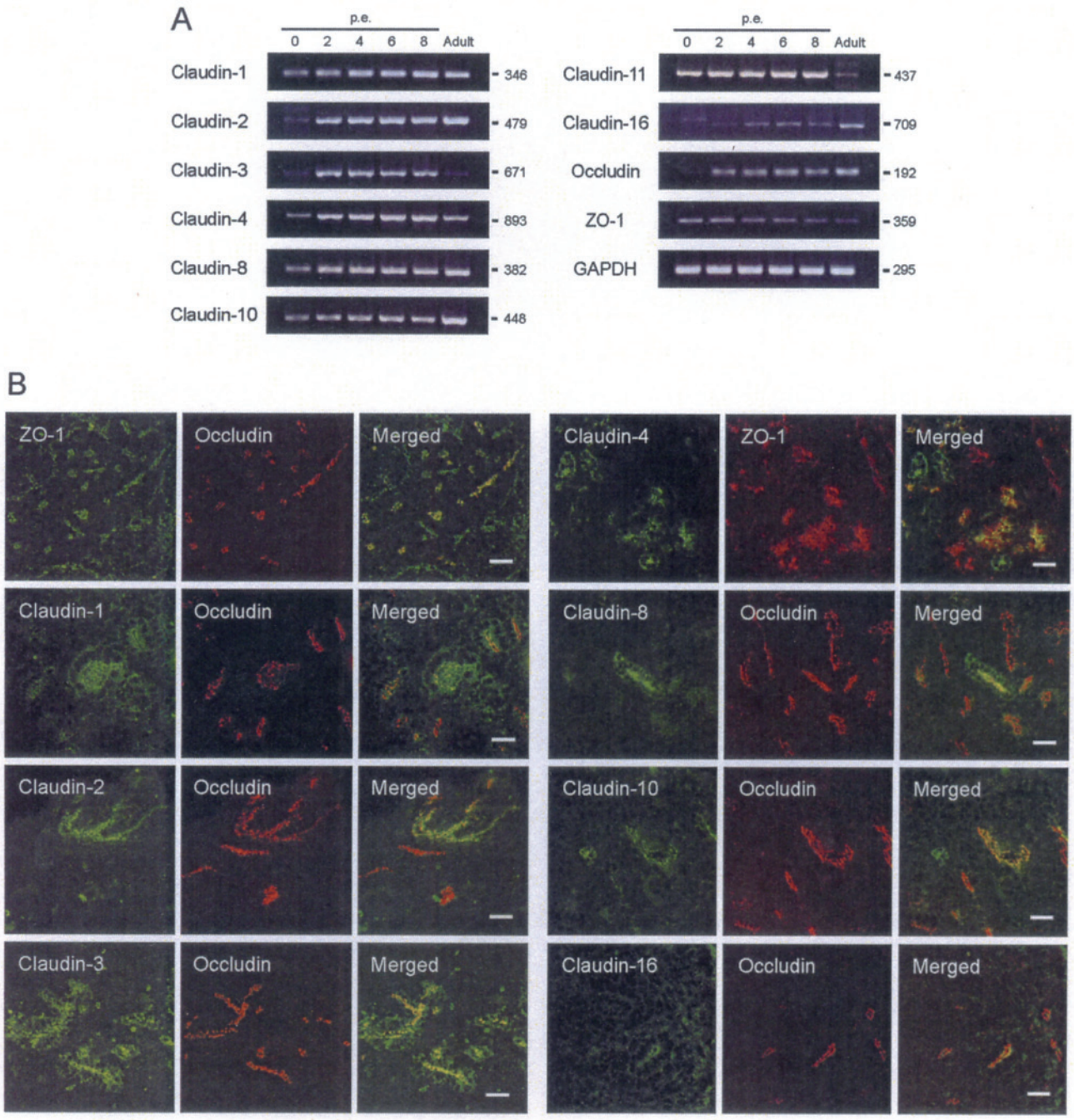
A
p.e.
0 2 4 6 8 Adult
Claudin-1
Claudin-2
Claudin-3
Claudin-4
Claudin-8
Claudin-10
346
479
671
893
382
448
p.e.
0 2 4 6 8 Adult
Claudin-11
Claudin-16
Occludin
ZO-1
GAPDH
437
709
192
359
295
B
ZO-1
Occludin
Merged
Claudin-4
ZO-1
Merged
Claudin-1
Occludin
Merged
Claudin-8
Occludin
Merged
Claudin-2
Occludin
Merged
Claudin-10
Occludin
Merged
Claudin-3
Occludin
Merged
Claudin-16
Occludin
Merged

Figure 13. Expression of the TJ proteins in cultured metanephroi. *A*, RT-PCR analyses for claudins (claudins 1-4, 8, 10, 11, and 16), occludin, and ZO-1 in metanephroi at p.e.0 through p.e.8 were performed as described in the legend for Fig. 1. PCR products for GAPDH are also shown. Product sizes are indicated in bp. A representative result of two independent experiments is shown. *B*, immunofluorescence microscopy for TJ proteins. Claudins 1-3, 8, 10, and 16, and ZO-1 were detected with pAbs specific to each protein and counterstained with the anti-occludin mAb. Claudin-4 was reacted with anti-claudin-4 mAb and then stained with anti-ZO-1 pAb. Specificities of antibodies to claudins 1-4 and 16 were confirmed by disappearance of immunofluorescent signals when the recombinant C-terminal peptide of each claudin tagged with glutathione S-transferase was included in the reactions as described previously (Chapter I). Bars = 20 μm.

DISCUSSION

The present study in this Chapter demonstrated that mouse E12 metanephroi could grow up to 8 days with the expression of claudin proteins and occludin and ZO-1 as well at the TJ in tubular epithelial cells. The most characteristic finding was that claudins 2, 10, and 16 were abundant at p.e.2, followed by increases during the incubation period, preceded by the expression of other claudins such as claudins 3, 4, and 8 (Figs. 11 and 13). These differences in expression patterns among claudin subtypes seem to be representative of the spatial and periodical processes of renal branching morphogenesis, the formation of branched epithelial tubules, at later stages of kidney development [62] that leads to the segment-specific distributions of claudins found in the mouse nephron [14]. That is, claudins 3, 4, and 8 are abundant in collecting tubules in the developed kidney, while the others distribute to proximal tubules (claudins 2 and 10) or the TAL of Henle's loop (claudins 16 and 10) formed by branching of the ureteric bud and its daughter collecting duct and the concomitant metanephric tubule formation [62]. These findings indicate that the expression patterns of specific claudin genes in cultured metanephroi are comparable to the developmental changes in the expression of the TJ proteins, including various claudin subtypes in normal embryonic kidneys.

Mutations and targeted disruptions of some specific claudin genes are known to cause pathological phenotypes in humans and animals. Disruption of the claudin-11 gene causes a neurological deficit due to the absence of TJs in central nervous system myelin in mice [45]. Human patients with *CLDN14* mutations [55] and *Cldn14* knockout mice [46] demonstrate inherited deafness due to cochlear hair cell

degeneration. Various mutations of the *CLDN16* gene are responsible for familial hypomagnesemia with hypercalciuria and nephrocalcinosis in the human [15] and renal tubular dysplasia with interstitial nephritis in cattle [19, 20]. While altered ionic permeability of the paracellular barrier of the reticular lamina due to the absence of claudin-14 is suspected to cause prolonged depolarization and eventual death of outer hairy cells leading to deafness [46], pathogeneses in other diseases, including renal tubular dysplasia in cattle, are unknown. Pathological findings including tubular atrophy and extensive interstitial nephritis in cattle at ages as young as 2-3 months suggested that tubular dysplasia is the primary change [22, 41], and thus claudin-16 would have some role in developmental formation of renal tubules in addition to selective paracellular transport of divalent cations. However, our pathological studies on *CLDN16*$^{-/-}$ bovine fetuses clearly demonstrated that the total lack of claudin-16 dose not affect renal tubular development and suggested that the pathogenesis of claudin-16 deficiency in cattle involves dysfunction of TJ strands in the TAL segment in paracellular transport (Chapter II). Therefore, some new approaches are desirable to clarify the roles of claudin-16 in the kidney.

One approach used by several groups to study the function of claudins has been to express individual claudins in monolayers of MDCK or LLC-PK1 cells. A major limitation of this approach is that the cells already express a background of multiple claudins. Since heterogeneous claudins form individual TJ strands as heteropolymers and claudin molecules adhere to each other in both homotypic and heterotypic manner, at the cell-cell interface [25], one cannot define a specific unit for an individual claudin in the function for intercellular adhesion and/or permeability barrier [3]. Actually, experimental data from several groups [47, 49], including ourselves, gave some

discrepancy on the function of claudin-16 in paracellular transport, as discussed in Chapter II.

The data presented above demonstrate that organotypic cultures of mouse metanephric explants have the ability to develop normally with regard to the expression of claudins, and thus the metanephroi are suitable to investigate the physiological and pathological roles of claudins in paracellular pathway as well as those in renal tubular formation. Further studies will involve applications of antisense oligonucleotides or interfering RNAs to the metanephroi as reported previously [59, 60] to repress specific claudin genes, including the *CLDN16* gene to analyze changes in paracellular permeability in the TAL segment. The only disadvantage of this organ culture is the difficulty in identification of developing tubular segments with generally utilized marker proteins as described above.

In conclusion, this study demonstrates developmental changes in the expression of the TJ protein claudins in cultured metanephroi representing those in embryonic kidneys, and thus suggests that the mouse metanephros is suitable to examine the functions of claudin-16 and other claudin species expressed in the kidney.

SUMMARY

Claudins are the major constituents of tight junction (TJ) strands and participate in the cell-cell adhesion and permeability barrier in epithelial cell layers. To investigate the suitability of metanephroi for analysis of the function of the TJ protein claudins, mouse metanephroi from embryos at day 12 of gestation were cultured and expression of claudins was compared with that in embryonic kidneys. During *in vitro* culture for 8 days, the metanephroi showed expression patterns very similar to those observed in embryonic kidneys in reverse transcription-polymerase chain reaction for the claudins examined, including claudins 1-4, 8, 10, 11, and 16, and the TJ proteins occludin and ZO-1. Immunofluorescence microscopy for claudins 1-4, 8, 10, and 16 showed localization of these claudins at the TJ with occludin and ZO-1 in some restricted tubular segments. These findings indicate that the metanephroi show developmental changes in the expression of the TJ protein claudins, representing those in embryonic kidneys, and thus suggest that the mouse metanephros is suitable to examine the functions of specific claudins in the kidney.

GENERAL CONCLUSION

Claudins are the major constituents of tight junction (TJ) strands and participate in the cell-cell adhesion and permeability barrier in epithelial cell layers. Now, claudins consist of a family of more than 20 homologous subtypes, and they show tissue-specific and segment-specific distribution patterns in epithelia such as those of the gastrointestinal tract and renal tubules. Among these claudin proteins, claudin-16 has been shown to be responsible for familial hypomagnesemia with hypercalciuria and nephrocalcinosis (FHHNC) in the human, and claudin-16 is likely to form aqueous pores that function as the paracelluar pathway for Mg^{2+} and Ca^{2+} in claudin-based TJs. Claudin-16 is also responsible for renal tubular dysplasia with interstitial nephritis in Japanese black cattle [19]. This disease is characterized by renal failure due to renal tubular dysplasia, and, in contrast to FHHNC, decreases in serum Mg^{2+} and Ca^{2+} concentrations are not apparent in affected cattle. The purpose of this study is to explore the molecular pathobiology of claudin-16 deficiency.

Although claudin-16 had been reported to be exclusively expressed in the thick ascending limb of Henle's loop (TAL) of human and murine kidneys, localization of claudin-16, as well as other claudin molecules, in bovine renal tubular segments has not been determined. As the first step to clarify the roles of claudin-16, in Chapter I, the expression and distribution of claudin-16 and several other major claudin subtypes, claudins 1-4 and 10, in bovine renal tubular segments were examined by immunofluorescence microscopy. Claudin-16 was exclusively distributed to the TJ in the tubular segment positive for Tamm-Horsfall glycoprotein, the TAL of Henle's loop, and was found co-localized with claudins 3, 4, and 10. Chapter I also demonstrates that

bovine kidneys possess segment-specific expression patterns for claudins 1-4 and 10 that are similar to those reported for mice, but has some differences. Particularly, distribution of claudin-4 in the TAL and distal convoluted tubules was characteristic of bovine nephrons. These findings demonstrated that the total lack of claudin-16 in the TAL segment is the sole cause of renal tubular dysplasia in cattle and suggested that the total lack of claudin-16 cause abnormal tubular development during the prenatal stage.

Next, to examine the prenatal pathogenesis in the claudin-16 deficiency, *CLDN16*$^{-/-}$ bovine fetuses at embryonic days 100, 180, and 270 were generated by embryo transfer, and the tubular formation and the expression of the tight junction proteins, including claudins 16, 1-4, 10, and 11, and occludin, during prenatal stages were examined in Chapter II. The *CLDN16*$^{-/-}$ fetuses showed no histological abnormality compared with normal *CLDN16*$^{+/+}$ fetuses even at 270 days of gestation. Claudins 3, 4, and 10 were constitutively distributed at the TJ of the TAL of Henle's loop, where claudin-16 was exclusively distributed, in the kidneys of *CLDN16*$^{-/-}$ fetuses as in normal *CLDN16*$^{+/+}$ kidneys. Distributions of claudins 3, 4, and 10 were also found at the TAL regions in the kidney with tubular dysplasia from a 7-month-old *CLDN16*$^{-/-}$ animal. These findings demonstrated that deficiency of claudin-16 did not cause apparent morphological abnormality in renal tubules during the period of renal development *in utero*. Thus, claudin-16 appears necessary for the maintenance of normal tubular architecture after birth presumably by its function of paracellular transport mechanism.

To clarify the roles of claudin-16 in the maintenance of tubular structures, establishment of experimental systems that mimic the nephrogenesis *in vivo* and expression of specific genes can be regulated is desirable. Organotypic culture of metanephric explants seem to be an adequate model for the studies on the functions of

claudin-16 in renal development and paracellular transport, since various studies have shown that mouse metanephroi removed from embryos continue to develop *in vitro* and display many of the processes of nephron induction and differentiation that are observed *in vivo* and the expression of specific genes can be inhibited in the presence of antisense oligonucleotides and/or interfering RNAs. In Chapter III, to investigate the suitability of metanephroi, mouse metanephroi from embryos at day 12 of gestation were cultured and expression of claudins was compared with that in embryonic kidneys. During *in vitro* culture for 8 days, the metanephroi showed expression patterns very similar to those observed in embryonic kidneys in reverse transcription-polymerase chain reaction for the claudins examined, including claudins 1-4, 8, 10, 11, and 16, and the TJ proteins occludin and ZO-1. Immunofluorescence microscopy for claudins 1-4, 8, 10, and 16 showed localization of these claudins at the TJ with occludin and ZO-1 in some restricted tubular segments. These findings indicate that the metanephroi show developmental changes in the expression of the TJ protein claudins, representing those in embryonic kidneys, and thus suggest that the mouse metanephros is suitable to examine the functions of specific claudins in the kidney.

In conclusion, the present study demonstrate that the total lack of claudin-16, that has exclusively restricted expression in the TAL segment in normal bovine kidney, is the sole cause of inherited renal tubular dysplasia in Japanese black cattle. This study evidently show that the lack of claudin-16 dose not affect renal tubular development in the prenatal stage, indicating that claudin-16 is indispensable for the maintenance of tubular architecture because of it's paracellualr transport mechanism that remains to be clarified.

REFERENCES

1. Anderson JM: Molecular structure of tight junctions and their role in epithelial transport. *News Physiol Sci* 16:126-130, 2001
2. Anderson JM, Van Itallie CM: Tight junctions and the molecular basis for regulation of paracellular permeability. *Am J Physiol* 269:G467-475, 1995
3. Van Itallie CM, Anderson JM: The molecular physiology of tight junction pores. *Physiology (Bethesda)* 19:331-338, 2004
4. Gumbiner BM: Breaking through the tight junction barrier. *J Cell Biol* 123:1631-1633, 1993
5. Schneeberger EE, Lynch RD: Structure, function, and regulation of cellular tight junctions. *Am J Physiol* 262:L647-661, 1992
6. Tsukita S, Furuse M: Pores in the wall: claudins constitute tight junction strands containing aqueous pores. *J Cell Biol* 149:13-16, 2000
7. Staehelin LA: Structure and function of intercellular junctions. *Int Rev Cytol* 39:191-283, 1974
8. Morita K, Furuse M, Fujimoto K, *et al.*: Claudin multigene family encoding four-transmembrane domain protein components of tight junction strands. *Proc Natl Acad Sci U S A* 96:511-516, 1999
9. Furuse M, Hirase T, Itoh M, *et al.*: Occludin: a novel integral membrane protein localizing at tight junctions. *J Cell Biol* 123:1777-1788, 1993
10. Ando-Akatsuka Y, Saitou M, Hirase T, *et al.*: Interspecies diversity of the occludin sequence: cDNA cloning of human, mouse, dog, and rat-kangaroo homologues. *J Cell Biol* 133:43-47, 1996
11. Saitou M, Fujimoto K, Doi Y, *et al.*: Occludin-deficient embryonic stem cells can differentiate into polarized epithelial cells bearing tight junctions. *J Cell Biol* 141:397-408, 1998
12. Furuse M, Fujita K, Hiiragi T, *et al.*: Claudin-1 and -2: novel integral membrane proteins localizing at tight junctions with no sequence similarity to occludin. *J Cell Biol* 141:1539-1550, 1998
13. Rahner C, Mitic LL, Anderson JM: Heterogeneity in expression and subcellular localization of claudins 2, 3, 4, and 5 in the rat liver, pancreas, and gut. *Gastroenterology* 120:411-422, 2001
14. Kiuchi-Saishin Y, Gotoh S, Furuse M, *et al.*: Differential expression patterns of claudins, tight junction membrane proteins, in mouse nephron segments. *J Am Soc*

Nephrol 13:875-886, 2002

15. Simon DB, Lu Y, Choate KA, *et al.*: Paracellin-1, a renal tight junction protein required for paracellular Mg2+ resorption. *Science* 285:103-106, 1999
16. Konrad M, Schlingmann KP, Gudermann T: Insight into the molecular nature of magnesium homeostasis. *Am J Physiol Renal Physiol* 286:F599-F605, 2004
17. Unwin RJ, Capasso G, Shirley DG: An overview of divalent cation and citrate handling by the kidney. *Nephron Physiol* 98:p15-20, 2004
18. Blanchard A, Jeunemaitre X, Coudol P, *et al.*: Paracellin-1 is critical for magnesium and calcium reabsorption in the human thick ascending limb of Henle. *Kidney Int* 59:2206-2215, 2001
19. Hirano T, Kobayashi N, Itoh T, *et al.*: Null mutation of PCLN-1/Claudin-16 results in bovine chronic interstitial nephritis. *Genome Res* 10:659-663, 2000
20. Ohba Y, Kitagawa H, Kitoh K, *et al.*: A deletion of the paracellin-1 gene is responsible for renal tubular dysplasia in cattle. *Genomics* 68:229-236, 2000
21. Hirano T, Hirotsune S, Sasaki S, *et al.*: A new deletion mutation in bovine Claudin-16 (CL-16) deficiency and diagnosis. *Anim Genet* 33:118-122, 2002
22. Sasaki Y, Kitagawa H, Kitoh K, *et al.*: Pathological changes of renal tubular dysplasia in Japanese black cattle. *Vet Rec* 150:628-632, 2002
23. Weber S, Schneider L, Peters M, *et al.*: Novel paracellin-1 mutations in 25 families with familial hypomagnesemia with hypercalciuria and nephrocalcinosis. *J Am Soc Nephrol* 12:1872-1881, 2001
24. Ohba Y, Kitoh K, Nakamura H, *et al.*: Renal reabsorption of magnesium and calcium by cattle with renal tubular dysplasia. *Vet Rec* 151:384-387, 2002
25. Furuse M, Sasaki H, Tsukita S: Manner of interaction of heterogeneous claudin species within and between tight junction strands. *J Cell Biol* 147:891-903, 1999
26. Furuse M, Furuse K, Sasaki H, *et al.*: Conversion of zonulae occludentes from tight to leaky strand type by introducing claudin-2 into Madin-Darby canine kidney I cells. *J Cell Biol* 153:263-272, 2001
27. Tsukita S, Furuse M, Itoh M: Multifunctional strands in tight junctions. *Nat Rev Mol Cell Biol* 2:285-293, 2001
28. Kim GH, Masilamani S, Turner R, *et al.*: The thiazide-sensitive Na-Cl cotransporter is an aldosterone-induced protein. *Proc Natl Acad Sci U S A* 95:14552-14557, 1998
29. Inaba M, Maede Y: Na,K-ATPase in dog red cells. Immunological identification and maturation-associated degradation by the proteolytic system. *J Biol Chem* 261:16099-16105, 1986
30. Agre P: Homer W. Smith award lecture. Aquaporin water channels in kidney. *J Am*

Soc Nephrol 11:764-777, 2000

31. Vandewalle A, Cluzeaud F, Bens M, *et al.*: Localization and induction by dehydration of ClC-K chloride channels in the rat kidney. *Am J Physiol* 272:F678-688, 1997
32. Yoshikawa M, Uchida S, Yamauchi A, *et al.*: Localization of rat CLC-K2 chloride channel mRNA in the kidney. *Am J Physiol* 276:F552-558, 1999
33. Hession C, Decker JM, Sherblom AP, *et al.*: Uromodulin (Tamm-Horsfall glycoprotein): a renal ligand for lymphokines. *Science* 237:1479-1484, 1987
34. Fushimi K, Uchida S, Hara Y, *et al.*: Cloning and expression of apical membrane water channel of rat kidney collecting tubule. *Nature* 361:549-552, 1993
35. Acharya P, Beckel J, Ruiz WG, *et al.*: Distribution of the tight junction proteins ZO-1, occludin, and claudin-4, -8, and -12 in bladder epithelium. *Am J Physiol Renal Physiol* 287:F305-318, 2004
36. Li WY, Huey CL, Yu AS: Expression of claudin-7 and -8 along the mouse nephron. *Am J Physiol Renal Physiol* 286:F1063-1071, 2004
37. Peppi M, Ghabriel MN: Tissue-specific expression of the tight junction proteins claudins and occludin in the rat salivary glands. *J Anat* 205:257-266, 2004
38. Inai T, Kobayashi J, Shibata Y: Claudin-1 contributes to the epithelial barrier function in MDCK cells. *Eur J Cell Biol* 78:849-855, 1999
39. McCarthy KM, Francis SA, McCormack JM, *et al.*: Inducible expression of claudin-1-myc but not occludin-VSV-G results in aberrant tight junction strand formation in MDCK cells. *J Cell Sci* 113 Pt 19:3387-3398, 2000
40. Van Itallie C, Rahner C, Anderson JM: Regulated expression of claudin-4 decreases paracellular conductance through a selective decrease in sodium permeability. *J Clin Invest* 107:1319-1327, 2001
41. Okada K, Ishikawa N, Fujimori K, *et al.*: Abnormal development of nephrons in claudin-16-defective Japanese black cattle. *J Vet Med Sci* 67:171-178, 2005
42. Hirayama H, Kageyama S, Moriyasu S, *et al.*: Genetic diagnosis of claudin-16 deficiency and sex determination in bovine preimplantation embryos. *J Reprod Dev* 50:613-618, 2004
43. Nitta T, Hata M, Gotoh S, *et al.*: Size-selective loosening of the blood-brain barrier in claudin-5-deficient mice. *J Cell Biol* 161:653-660, 2003
44. Furuse M, Hata M, Furuse K, *et al.*: Claudin-based tight junctions are crucial for the mammalian epidermal barrier: a lesson from claudin-1-deficient mice. *J Cell Biol* 156:1099-1111, 2002
45. Gow A, Southwood CM, Li JS, *et al.*: CNS myelin and sertoli cell tight junction strands are absent in Osp/claudin-11 null mice. *Cell* 99:649-659, 1999

46. Ben-Yosef T, Belyantseva IA, Saunders TL, *et al.*: Claudin 14 knockout mice, a model for autosomal recessive deafness DFNB29, are deaf due to cochlear hair cell degeneration. *Hum Mol Genet* 12:2049-2061, 2003

47. Hou J, Paul DL, Goodenough DA: Paracellin-1 and the modulation of ion selectivity of tight junctions. *J Cell Sci* 118:5109-5118, 2005

48. Shareghi GR, Agus ZS: Magnesium transport in the cortical thick ascending limb of Henle's loop of the rabbit. *J Clin Invest* 69:759-769, 1982

49. Ikari A, Hirai N, Shiroma M, *et al.*: Association of paracellin-1 with ZO-1 augments the reabsorption of divalent cations in renal epithelial cells. *J Biol Chem* 279:54826-54832, 2004

50. Kokot F, Dulawa J: Tamm-Horsfall protein updated. *Nephron* 85:97-102, 2000

51. Serafini-Cessi F, Malagolini N, Cavallone D: Tamm-Horsfall glycoprotein: biology and clinical relevance. *Am J Kidney Dis* 42:658-676, 2003

52. Fasth A, Hoyer JR, Seiler MW: Renal tubular immune complex formation in mice immunized with Tamm-Horsfall protein. *Am J Pathol* 125:555-562, 1986

53. Hoyer JR: Tubulointerstitial immune complex nephritis in rats immunized with Tamm-Horsfall protein. *Kidney Int* 17:284-292, 1980

54. Mayrer AR, Kashgarian M, Ruddle NH, *et al.*: Tubulointerstitial nephritis and immunologic responses to Tamm-Horsfall protein in rabbits challenged with homologous urine or Tamm-Horsfall protein. *J Immunol* 128:2634-2642, 1982

55. Wilcox ER, Burton QL, Naz S, *et al.*: Mutations in the gene encoding tight junction claudin-14 cause autosomal recessive deafness DFNB29. *Cell* 104:165-172, 2001

56. Avner ED, Piesco NP, Sweeney WE, Jr., *et al.*: Renal epithelial development in organotypic culture. *Pediatr Nephrol* 2:92-99, 1988

57. Maeshima A, Yamashita S, Maeshima K, *et al.*: Activin a produced by ureteric bud is a differentiation factor for metanephric mesenchyme. *J Am Soc Nephrol* 14:1523-1534, 2003

58. Nagata M, Watanabe T: Podocytes in metanephric organ culture express characteristic in vivo phenotypes. *Histochem Cell Biol* 108:17-25, 1997

59. Quaggin SE, Yeger H, Igarashi P: Antisense oligonucleotides to Cux-1, a Cut-related homeobox gene, cause increased apoptosis in mouse embryonic kidney cultures. *J Clin Invest* 99:718-724, 1997

60. Davies JA, Ladomery M, Hohenstein P, *et al.*: Development of an siRNA-based method for repressing specific genes in renal organ culture and its use to show that the Wt1 tumour suppressor is required for nephron differentiation. *Hum Mol Genet* 13:235-246, 2004

61. Takada K, Takiguchi M, Konno A, *et al.*: Autoimmunity against a tissue kallikrein in IQI/Jic Mice: a model for Sjogren's syndrome. *J Biol Chem* 280:3982-3988, 2005

62. Piscione TD, Rosenblum ND: The molecular control of renal branching morphogenesis: current knowledge and emerging insights. *Differentiation* 70:227-246, 2002

ACKNOWLEDGMENTS

I express my sincere gratitude to Professor Mutsumi Inaba (Laboratory of Molecular Medicine, Department of Veterinary Clinical Sciences, Graduate School of Veterinary Medicine, Hokkaido University) for his excellent supervision throughout this work.

I am also gratitude to Professor Takashi Umemua (Laboratory of Comparative Pathology, Department of Veterinary Clinical Sciences, Graduate School of Veterinary Medicine, Hokkaido University), Professor Yasuhiro Kon (Laboratory of Anatomy, Department of Biomedical Science, Graduate School of Veterinary Medicine, Hokkaido University), and Associate Professor Toru Ishikawa (Laboratory of Physiology, Department of Biomedical Science, Graduate School of Veterinary Medicine, Hokkaido University) for their constructive and helpful advice on this study.

I extend my heartful appreciation to Professor Mitsuyoshi Takiguchi (Department of Small Animal Clinical Science, School of Veterinary Medicine, Rakuno Gakuen University) for comprehensive advice and continuous encouragement, and Drs. S. Kageyama, H. Hirayama, S. Onoe, S. Moriyasu, K. Sawai, and A. Minamihashi (Hokkaido Animal Research Center, Shintoku, Japan) for their technical support, Drs. A. Takasuga and Y. Sugimoto (Shirakawa Institute of Animal Genetics, Fukushima, Japan) for the anti-claudin-16 antibody, Dr. M. A. Knepper (Laboratory of Kidney and Electrolyte Metabolism, National Institute of Health, Bethesda, MD, USA) for the anti-NCCT antibody.

I really enjoyed to work with cheerful and pleasant members of Laboratory of Molecular Medicine.

My special thanks to my father, Kenji Ohta, for his thoughtfulness and understanding.

和 文 要 約

黒毛和種牛腎尿細管形成不全症（クローディン-16 欠損症）の分子病態

大田　寛

北海道大学大学院獣医学研究科・診断治療学講座・臨床分子生物学教室

クローディンは、上皮細胞のタイトジャンクション(TJ)を構成する主要な膜内在性蛋白質である。現在20種を超えるクローディンサブタイプが知られ、これらが組織特異的に分布し、TJ における細胞間隙の選択的な物質透過性と細胞間接着を担っている。クローディン-16 は、ヒト家族性低マグネシウム血症高カルシウム尿症(FHHNC)の原因遺伝子産物として同定され、腎尿細管における二価陽イオンの傍細胞輸送に関与すると推定されている。一方、クローディン-16 遺伝子(*CLDN16*)の完全欠損による黒毛和種牛の腎尿細管形成不全症の主徴は尿細管の異形成による腎機能低下であり二価陽イオンの代謝異常は顕著ではない。本研究では、牛クローディン-16 欠損症発症の分子基盤の解明を目的とし、牛クローディン-16 の腎尿細管における局在、ならびに尿細管形成における機能の解析をおこなった。

クローディン-16 はヒトおよびマウスの腎尿細管において、ヘンレの太い上行脚部(TAL)に特異的に発現することが明らかとなっているが、牛腎尿細管分節におけるクローディン-16 ならびに他のクローディンサブタイプの局在は明らかでない。そこで、まず、蛍光抗体法を用い牛腎尿細管におけるクローディン-16 の分布、ならびにそれと共在するクローディン分子種の同定を行った。その結果、牛クローディン-16 は、Tamm-Horsfall 糖蛋白質(THP)陽性の尿細管、即ち、TAL の TJ 領域に限定して存在することが明らかになった。また、他のクローデ

ィン分子群は、従来知られるマウス腎とは若干異なる分節特異的な分布を示し、特に牛腎尿細管においてクローディン-4 が TAL および遠位尿細管に発現することが明らかとなった。これらのことより、牛腎尿細管においてクローディン-16 は TAL に特異的に発現し、同分節でクローディン-3、-4、ならびに-10 と共在し TJ を形成することが判明した。

牛クローディン-16 欠損症の病態から、クローディン-16 が尿細管形成過程において重要な機能を有し、その欠損が胎生期の尿細管形成を障害することが推定される。そこで、クローディン-16 欠損症牛の胎生期における腎尿細管形成過程を解析する目的で、北海道立畜産試験場との共同研究で、*CLDN16-/-*胚の受精卵移植によりクローディン-16 を欠損した胎子を作出し、その胎生期における腎尿細管の組織構築を *CLDN16+/+*個体における腎と比較した。*CLDN16+/+*では胎生 100 日齢で特定の尿細管上皮の管腔側にクローディン-16, 3, 4, ならびに 10 の分布が認められた。*CLDN16-/-*胎子もクローディン-16 の欠損以外は全く同様の組織構造がみられ、100 日齢、あるいは出生直前の 270 日齢の腎でも THP 陽性でクローディン-3, 4, 10 が共在する明瞭な尿細管構造が認められた。この時期の *CLDN16-/-*腎では尿細管構造の乱れはみとめられず、他の主要クローディン分子群の RNA、ならびに蛋白質の発現量も正常胎子との相違はみられなかった。これらのことから、クローディン-16 欠損は尿細管組織構築自体には何ら影響しないことが明らかとなった。これらの結果から、クローディン-16 の欠損は TAL を構成する上皮細胞間の TJ の選択的な物質透過性の異常をきたし、出生後の尿細管構築崩壊に関わることが推定された。

この仮説を実証するモデルのひとつとして、マウス胎子後腎の器官培養系が有用と考えられた。そこで、妊娠 12 日目のマウス胎子から得た後腎を器官培養して、クローディン分子群(クローディン 1-4, 8, 10, 11, 16)、ならびに同じ

くTJタンパク質であるオクルーディンとZO-1の発現動態をRT-PCR法と蛍光抗体法で解析し、胎子腎の発達過程と比較・検討した。8日間の培養期間中、後腎におけるクローディン-16をはじめとするクローディン分子群のmRNA発現量は、胎子腎の発達過程にみられるのと同様の、個々の分子に特徴的な変動を示した。また、蛍光抗体法での観察では、各クローディン分子が特定の尿細管の上皮細胞管腔側にオクルーディン、ZO-1と局在をともにすること、即ちTJ領域に分布することが示された。これらの結果より、マウス後腎の器官培養が、胎子腎の発達にともなったクローディン分子群の発現動態を再現できる有用なモデルであることが示唆された。

以上のように、本研究からクローディン-16が牛腎尿細管TALに特異的に発現すること、その欠損は胎生期の尿細管組織構築形成自体には影響を及ぼさないことが明らかになった。この結果は、黒毛和種牛におけるクローディン-16欠損による腎尿細管形成不全症の発症が出生後の尿細管上皮細胞の崩壊によることを明らかに示すとともに、それがクローディン-16の欠損によるTAL領域尿細管における管腔側—基底側内イオン分布のバランスの異常に起因する可能性を示唆するものである。さらに本研究は、その実証に、マウス後腎の器官培養系が有用となる可能性を示した。